PASJ: Publ. Astron. Soc. Japan **62**, 19–37, 2010 February 25

Subaru FOCAS Spectroscopic Observations of High-Redshift Supernovae*

Tomoki MOROKUMA,[1,†] Kouichi TOKITA,[2] Christopher LIDMAN,[3] Mamoru DOI,[2,4] Naoki YASUDA,[4,5] Greg ALDERING,[6] Rahman AMANULLAH,[6,7] Kyle BARBARY,[6] Kyle DAWSON,[8] Vitaliy FADEYEV,[9] Hannah K. FAKHOURI,[6] Gerson GOLDHABER,[6] Ariel GOOBAR,[7] Takashi HATTORI,[10] Junji HAYANO,[2] Isobel M. HOOK,[11,12] D. Andrew HOWELL,[13,14] Hisanori FURUSAWA,[1] Yutaka IHARA,[2,†] Nobunari KASHIKAWA,[1] Rob A. KNOP,[15] Kohki KONISHI,[5] Joshua MEYERS,[6] Takeshi ODA,[16] Reynald PAIN,[17] Saul PERLMUTTER,[6] David RUBIN,[6] Anthony L. SPADAFORA,[6] Nao SUZUKI,[6] Naohiro TAKANASHI,[1] Tomonori TOTANI,[16] Hiroyuki UTSUNOMIYA,[2] and Lifan WANG[18] (Supernova Cosmology Project)

[1]*National Astronomical Observatory of Japan, 2-21-1 Osawa, Mitaka, Tokyo 181-8588*
tomoki.morokuma@nao.ac.jp
[2]*Institute of Astronomy, Graduate School of Science, The University of Tokyo, 2-21-1 Osawa, Mitaka, Tokyo 181-0015*
[3]*Oskar Klein Centre, Stockholm University, AlbaNova University Centre, 10691 Stockholm, Sweden*
[4]*Institute of Physics and Mathematics of the Universe, The University of Tokyo, Kashiwa, Chiba 277-8582*
[5]*Institute for Cosmic Ray Research, The University of Tokyo, Kashiwa, Chiba 277-8582*
[6]*Lawrence Berkeley National Laboratory, 1 Cyclotron Road, Berkeley, CA 94720, USA*
[7]*Physics Department, Stockholm University, AlbaNova University Centre, 10691 Stockholm, Sweden*
[8]*Department of Physics and Astronomy, University of Utah, Salt Lake City, UT 84112, USA*
[9]*Santa Cruz Institute for Particle Physics, University of Californica, Santa Cruz, CA 94064, USA*
[10]*Subaru Telescope, National Astronomical Observatory of Japan, 650 North A'ohoku Place, Hilo, HI 96720, USA*
[11]*Oxford Astrophysics, Department of Physics, Denys Wilkinson Building, Keble Road, Oxford OX1 3RH, UK*
[12]*INAF–Observatorio Astronomico di Roma, via Frascati 33, 00040, Monteporzio (RM), Italy*
[13]*Las Cumbres Observatory Global Telescope Network, 6740 Cortona Dr., Suite 102, Goleta, CA 93117, USA*
[14]*Department of Physics, University of California, Santa Barbara, Broida Hall, Mail Code 9530, Santa Barbara, CA 93106-9530, USA*
[15]*Department of Physics and Astronomy, Vanderbilt University, P.O. Box 1807, Nashville, TN 37240, USA*
[16]*Department of Astronomy, Kyoto University, Sakyo-ku, Kyoto 606-8502*
[17]*LPNHE, CNRS-IN2P3 and University of Paris VI and VII, 75005 Paris, France*
[18]*Physics Department, Texas A&M University, College Station, TX 77843, USA*

(Received 2009 July 31; accepted 2009 November 6)

Abstract

We present spectra of high-redshift supernovae (SNe) that were taken with the Subaru low-resolution optical spectrograph, FOCAS. These SNe were found in SN surveys with Suprime-Cam on Subaru, the CFH12k camera on the Canada-France-Hawaii Telescope, and the Advanced Camera for Surveys on the Hubble Space Telescope. These SN surveys specifically targeted $z > 1$ Type Ia supernovae (SNe Ia). From the spectra of 39 candidates, we obtained redshifts for 32 candidates and spectroscopically identified 7 active candidates as probable SNe Ia, including one at $z = 1.35$, which is the most distant SN Ia to be spectroscopically confirmed with a ground-based telescope. An additional 4 candidates were identified as likely SNe Ia from the spectrophotometric properties of their host galaxies. Seven candidates are not SNe Ia, either being SNe of another type or active galactic nuclei. When SNe Ia were observed within one week of the maximum light, we found that we could spectroscopically identify most of them up to $z = 1.1$. Beyond this redshift, very few candidates were spectroscopically identified as SNe Ia. The current generation of super red-sensitive, fringe-free CCDs will push this redshift limit higher.

Key words: cosmology: observations — stars: supernovae: general — surveys

1. Introduction

Type Ia supernovae (SNe Ia) have proven to be very good standard candles for cosmological studies. They are bright enough to detect at cosmological distances, $z \sim 1.5$, if one uses 8–10 m class ground-based optical telescopes or the Hubble Space Telescope (HST), and their luminosities can be standardised using empirical relations between the luminosity and the light curve shape (Phillips 1993) and colour (Tripp 1998).

SNe Ia have played a leading role in measuring the expansion history of the universe since two independent teams, the Supernova Cosmology Project (SCP) and the High-z Team, discovered an accelerating expansion of the universe (Perlmutter et al. 1999; Riess et al. 1998). Since then, many projects to discover and identify SNe Ia have been organized. For example, the Carnegie Supernova Project (CSP: Hamuy et al. 2006), the Nearby Supernova Factory (SNfactory: Aldering et al. 2002), the Harvard-Smithsonian Center for Astrophysics (CfA) supernova survey (Jha et al. 2006; Hicken

* Based on data collected at Subaru Telescope, which is operated by the National Astronomical Observatory of Japan.

† Research Fellow of the Japan Society for the Promotion of Science (JSPS).

Table 1. Summary of the SN candidate search campaigns.*

Campaign	Field	Telescope/Instrument	$N_{\rm pointings}$	Year/Month	Band	$N_{\rm epoch}$	$N_{\rm spec}$
Subaru 2001	CL1604_0,4	Subaru/Suprime-Cam	2	2001/04–2001/05	R_C	2	1
Subaru 2001	MS1520.1	Subaru/Suprime-Cam	1	2001/04–2001/05	i'	2	1
Subaru 2001	SDF	Subaru/Suprime-Cam	1	2001/04–2001/05	i'	2	5
Spring 2002	SDF	Subaru/Suprime-Cam	2	2002/04–2002/05	i'	2	0
Spring 2002	SDFe,SDFw	Subaru/Suprime-Cam	2	2002/04–2002/05	i'	2	0
Spring 2002	SS1,2,3,4	Subaru/Suprime-Cam	4	2002/03–2002/04	i'	3	1
Spring 2002	C02 fields	CFHT/CFH12k	3	2002/03–2002/06	I	$\sim$10	0
Fall 2002	SXDF	Subaru/Suprime-Cam	5	2002/09–2003/10	i'	5–7	2
HST Cluster SN	galaxy clusters	HST/ACS	25	2005/08–2006/08	z_{850}	5–10	8+5

* The campaign name and search fields are denoted in columns 1 and 2. The telescope and instrument used for the SN search, and the number of pointings are denoted in columns 3 and 4. The search season, the broad-band filter used in the search, the number of search epochs, and the number of spectra shown in this paper are denoted in columns 5, 6, 7, and 8, respectively. $N_{\rm spec}$ for HST Cluster Supernova Survey is the number of SN candidates and host galaxies.

et al. 2009), the Sloan Digital Sky Survey-II Supernova Survey (SDSS-II SN Survey: Sako et al. 2008; Frieman et al. 2008), the Supernova Legacy Survey (SNLS: Astier et al. 2006), the Equation of State: SupErNovae trace Cosmic Expansion (ESSENCE) survey (Miknaitis et al. 2007; Wood-Vasey et al. 2007), and the Higher-Z team (Riess et al. 2007) have detected around 1000 SNe up to redshift $z \sim 1.5$. The combination of SN Ia data with measurements of cosmic microwave background (CMB) fluctuations (Spergel et al. 2003, 2007; Komatsu et al. 2009), baryon acoustic oscillations (BAO: Eisenstein et al. 2005) and galaxy cluster number counts (Vikhlinin et al. 2009) have constrained the dark-energy equation of state parameter. However, the limits are consistent with very different dark-energy models, so the fundamental nature of dark energy remains unclear. It is currently one of the biggest mysteries in physics, and combined astronomical observations (SNe Ia, CMB, BAO, and weak lensing) seem to be the only way to constrain its properties.

Since the discovery of the accelerating expansion of the universe, the SCP has been carrying out imaging surveys for SNe Ia at $z \gtrsim 1$, an epoch during which the expansion of the universe is expected to be decelerating. Spectroscopic follow-up observations are an essential part of these surveys, providing spectroscopically determined redshifts and, when necessary and possible, direct confirmation of the SN type. In this paper, we present spectra of SNe and their host galaxies taken with the Faint Object Camera And Spectrograph (FOCAS: Kashikawa et al. 2002) on the Subaru 8.2-m telescope. Twelve SN candidates shown here were found in ground-based observations targeting blank fields and nearby galaxy clusters with Suprime-Cam (Miyazaki et al. 2002) on Subaru and the CFH12k camera (Cuillandre et al. 2000) on the Canada-France-Hawaii telescope (CFHT). The remaining 27 SN candidates were discovered using the Advanced Camera for Surveys (ACS: Benítez et al. 2003) on HST[1] targeting high-redshift galaxy clusters in a program called the HST Cluster SN Survey (Program number 10496, PI: Perlmutter). These SN searches specifically targeted $z > 1$ SNe Ia, for which there have been relatively few spectroscopically confirmed SNe Ia (Aldering et al. 1998; Coil et al. 2000; Tonry et al. 2003; Barris et al. 2004; Riess et al. 2004; Lidman et al. 2005; Riess et al. 2007). In section 2, we summarize the SN searches and present data for both imaging and spectroscopy. Spectroscopic data reductions are described in section 2. SN and host galaxy classifications are shown in section 3 and section 4, respectively. In section 5, we describe factors that influence the classification of SNe. Section 6 is a summary of the paper. We used the standard ΛCDM cosmological parameters of $(H_0, \Omega_M, \Omega_\Lambda) = (70,\ 0.27,\ 0.73)$ for calculating the age of the universe at a certain redshift. All magnitudes were measured in the AB system.

2. Observations and Data

The spectroscopic observations described in this paper were carried out during our SN campaigns, which were specifically targeting $z > 1$ SNe Ia. Each campaign generally consisted of broad-band imaging to discover SNe Ia, a spectroscopic follow-up to determine SN types and redshifts, and a photometric follow-up to measure light curves. To first find, and then effectively follow $z > 1$ SNe Ia, we used both wide-field imagers on ground-based telescopes, namely Suprime-Cam ($34' \times 27'$) on the Subaru telescope and the CFH12k camera ($42' \times 28'$) on CFHT, and ACS ($3\farcm3 \times 3\farcm3$) on HST. SN candidates shown in this paper were found during 2001, 2002, 2005, and 2006.

2.1. SN Search Campaigns

Our search for SNe Ia was conducted in a series of four campaigns. Three of these were conducted with ground-based facilities during the Northern Spring of 2001, the Northern Spring of 2002 and the Northern Fall of 2002. The fourth was an ACS search conducted during 2005 and 2006. Some campaigns consisted of multiple searches with several instruments. Details of the searches are given in table 1. Additional details can be found in Lidman et al. (2005), N. Yasuda et al. (in preparation), and Dawson et al. (2009), and are briefly summarised here. Some of the SN discoveries were reported

[1] Based on observations made with the NASA/ESA Hubble Space Telescope and obtained from the data archive at the Space Telescope Institute. STScI is operated by the Association of Universities for Research in Astronomy, Inc. under the NASA contract NAS 5-26555. The observations are associated with program 10496.

in IAU circulars (Doi et al. 2001; Yasuda et al. 2002; Doi et al. 2003; Dawson et al. 2006).

2.1.1. The Subaru 2001 campaign

The Subaru Suprime-Cam campaign conducted in the Spring of 2001 was a pilot search for later SN searches with this instrument. The relatively wide field-of-view and the high sensitivity provided by Suprime-Cam enabled the discovery of high-redshift SNe more effectively than ACS (Yasuda et al. 2003). Only two- or three-epochs were taken with Suprime-Cam, which means that these data were not, by themselves, enough to derive light curves, although one candidate was followed with WFPC2 on HST (R. Amanullah et al. in preparation). The search fields were centered on two galaxy clusters, CL 1604+4321 ($z = 0.90$: Lubin et al. 2004) and MS 1520.1+3002 ($z = 0.117$: Stocke et al. 1991), and several blank fields, such as the Subaru Deep Field (SDF: Kashikawa et al. 2004). The SDF observations were carried out as a part of the SDF project. The imaging data for the SN searches were obtained in either the R_C or i' filters. Typical exposure times and limiting magnitudes for each epoch were one hour and R_C, $i' \sim 26$ mag. SNe found in these campaigns are named [field]-[SN ID] or [field][SN ID].

The Suprime-Cam data are very useful for investigating SN rates, even though there are only 2 or 3 epochs. By combining Suprime-Cam data in Abell 2152 (Totani et al. 2005), Oda et al. (2008) obtained SN rates for both SNe Ia and core-collapse SNe, and by using a theoretical model that relates the SNe rate to the star-formation rate (Oda & Totani 2005), the cosmic star-formation history. This provides an estimate that is independent of galaxy studies. It also takes advantage of the fact that SNe can trace the star-formation activity, even though galaxies are either too diffuse or too faint to detect. Using well-sampled light curves from the SXDS data (Morokuma et al. 2008 and sub-subsection 2.1.3 of this paper), the cosmological evolution of the SN Ia rate can be measured (Totani et al. 2008; Y. Ihara et al., in preparation).

2.1.2. The Spring 2002 campaign

The Spring 2002 campaign consisted of four searches: two searches with Subaru, a CFHT search, and a CTIO search (Lidman et al. 2005). The two Subaru searches used Suprime-Cam, were done back-to-back and searched for SNe Ia in the SDF field, two fields surrounding the SDF field (SDFe and SDFw, which are to the east and west of the SDF, respectively), and four other blank fields (SS1, SS2, SS3, and SS4). The CFHT search was a rolling search, which was similar to one subsequently done by the SNLS (Astier et al. 2006), where each field was observed 3 to 4 times per lunation over a period of several lunations. These kinds of searches automatically provide well-sampled light curves of discovered transients. We did not follow CTIO candidates with FOCAS. SNe discovered in this search are reported in Lidman et al. (2005).

SN candidates found in this campaign were named S02-[SN ID] and C02-[SN ID] for the Subaru and CFHT searches, respectively. Followup imaging observations of several high-redshift SNe were obtained with HST/ACS and two ground based IR instruments: ISAAC (Infrared Spectrometer And Array Camera: Moorwood et al. 1998) on the VLT and NIRI (Near InfraRed Imager and Spectrometer: Hodapp et al. 2003) on Gemini-North. These observations will be reported in N. Suzuki et al. (in preparation).

2.1.3. The Fall 2002 campaign

In the Fall 2002 campaign, we took multi-epoch i'-band images of five fields with Suprime-Cam (N. Yasuda et al. in preparation). The fields were centered on the Subaru/XMM-Newton Deep Field (SXDF). The Subaru/XMM-Newton Deep Survey (SXDS) project (Sekiguchi et al. 2004; K. Sekiguchi in preparation) has taken deep multi-wavelength data, from X-ray to radio, of this region.

Compared to earlier Subaru campaigns, the search and follow-up of candidates discovered during the Fall 2002 campaign were more comprehensive. Reference images taken during the end of 2002 September were compared with search images that were taken during the beginning of 2002 November. The typical exposure time was one hour and the limiting magnitude was $i' \sim 26$ mag. The deep and wide-field Suprime-Cam data provided us with ~ 100 variable objects over a timescale of 1 month (Morokuma et al. 2008; N. Yasuda et al. in preparation). Follow-up imaging observations of several high-redshift SNe were carried out using HST/ACS in the optical and NICMOS (Near Infrared Camera and Multi-Object Spectrometer: Thompson et al. 1999) on HST in the near infrared. We also obtained ground-based near-infrared J-band imaging data of one candidate with both CISCO [Cooled Infrared Spectrograph and Camera for OH-airglow Suppressor (Iwamuro et al. 2001; Motohara et al. 2002)] on the Subaru telescope and VLT/ISAAC. These observations will be reported in N. Suzuki et al. (in preparation). SN candidates found in this campaign are named SuF02-[SN ID].

2.1.4. The HST cluster supernova survey

The HST Cluster Supernova Survey was conducted in 2005 and 2006 with ACS on HST (Dawson et al. 2009). The targeted fields were galaxy clusters at $0.9 < z < 1.5$. Galaxy clusters are rich in early-type galaxies, which are expected to have little dust. In current SN Ia cosmological studies, the systematic uncertainty in the correction for dust attenuation is comparable to statistical uncertainties. For example, it is not clear if the extinction law is universal or unevolving. The most straightforward way to avoid (or reduce) this systematic error is to find SNe Ia in dust-free environments. Also, the dispersion in the corrected peak B-band luminosity of SNe Ia in early-type galaxies is smaller than that in late-type galaxies (e.g., Takanashi et al. 2008). Therefore, we searched for SNe Ia in early-type galaxies by targeting galaxy clusters, which is an effective way of finding a large number of early type galaxies at high redshift in small fields of view. Another advantage in targeting early-type galaxies, where star-forming activities have been quenched, is that SNe found in such galaxies are expected to be SNe Ia with high probability, since there should be no core-collapse SNe in these galaxies.

In total, 25 high-redshift galaxy clusters were targeted. Typical exposure times and limiting magnitudes for each epoch were 30 minutes and F850LP (z_{850}) ~ 25 mag, respectively. The clusters were also observed using the ACS F775W (i_{775}) filter, and active high-redshift SNe were observed with the F110W filter on NICMOS. The SN candidates found in this campaign are named SCP[year][Cluster ID][SN ID], where "year" corresponds to the year of discovery, "Cluster ID" is a letter arbitrarily assigned to each cluster for scheduling

purposes, and "SN ID" is a number assigned to each SN within a cluster according to its time of discovery in the search.

2.2. FOCAS Follow-Up Spectroscopic Observations

Spectroscopic follow-up was used to obtain redshifts and, if the SN phase was near maximum light, the SN type. The candidates observed with FOCAS are summarized in tables 2 and 3. Spectroscopic follow-up was also done with other facilities, and reported elsewhere (Lidman et al. 2005; N. Yasuda et al. in preparation). During the Fall 2002 campaign, the Subaru telescope was used mainly for discovering SNe, so the number of SN candidates observed spectroscopically with FOCAS was small for this particular campaign.

We used the long slit mode of FOCAS until 2005 December, and then mainly the multi-object slit mode after that. There are two reasons for the change. First, candidates from the HST Cluster Supernova Survey campaign were faint, which increased the difficulty in acquiring these targets with the long slit mode. The multi-object slitmasks can be manufactured to include several alignment holes to catch bright stars within the FOCAS FOV (6′ diameter), thus enabling us to center targets more precisely. Slitmask observations also allow us to observe additional targets, such as cluster members, at the same time (Eisenhardt et al. 2008; Tanaka et al. 2008; Dawson et al. 2009; J. Meyers et al. in preparation). Also, improvements in the mask alignment software by the FOCAS instrument team allowed us to acquire targets more quickly. The slit widths were 0.″8 in most of the observations. When the seeing was poor, slit widths of 1.″0 were used. The atmospheric dispersion corrector was used in all observations. Combinations of grisms and order-sort filters were 300B and SY47, or 300R and SO58, which resulted in spectra covering the 4700–9000Å and 5800–10000Å regions, respectively. Each exposure lasted 20 to 30 minutes. The objects were dithered by several arcseconds over several positions along the slit in order to effectively remove bad pixels, cosmic rays, and detector fringes. The exposure times varied with the target brightness and the priority. Typically, the seeing was 0.″6 to 1.″0 and the total exposure times were 1–3 hours.

2.3. Spectroscopic Data Reduction

The FOCAS[2] spectroscopic data were reduced in a mostly standard way using the Image Reduction and Analysis Facility (IRAF[3]). The bias was removed by fitting a low-order polynomial to the overscan region, which lies parallel to the dispersion direction, and the flat-fielding was done with lamp flats. The background was removed while simultaneously masking bad pixels and bad columns, and correcting for detector fringing, except for those cases in which there were too few frames to compute a fringe correction. The flexure is small enough for one to use all of the data taken with the same configuration during a night to make fringe correction images. The 2d spectral data were then stacked, and the 1d spectrum of the object extracted. Wavelength calibration was done using night-sky emission lines. The flux scale was calibrated using the standard star spectrum obtained closest in time. BD + 28 4211, Feige 34, Feige 110, Hz 44, GD 71, G 191-B2B, LTT 2415, and Wolf 1346 were used as flux standards. Most of them are HST spectrophotometric standard stars with well-measured flux densities. We also removed strong telluric absorption features using the standard star data that was used for flux calibration; however, we note that these corrections are not perfect, and when presenting the spectra we mark the main regions that may be affected by telluric features.

Fringes, which can be significant at long wavelengths, were removed from the sky background to increase the signal-to-noise ratio of the spectra. To remove these fringe patterns effectively, we adopted an observational and data reduction strategy that is described below. The procedure is similar to that described in Lidman et al. (2005), which was used for data obtained with FORS1 and FORS2 on the VLT. The difference between ours and Lidman et al. (2005) comes from the specific properties (distortion, pixel scale, spectral resolution, and so on) of each instrument.

All observations were dithered by several arcseconds along the spatial direction of the slits, which were set perpendicular to the dispersion direction. In long slit spectroscopy, we used all of the exposures with the same configuration during a given night to create a fringe frame for that set up and that night. We also carefully designed slitmasks for SCP05D0 and SCP05D6 (D_mask1 and D_mask2), SCP05E12 (E_mask4 and E_mask6), and SCP05T1 (T_mask1 and T_mask2) so that the slit positions of these targets on the CCD were the same. Data were sorted with respect to the grism, slit width, date and location of the candidate on the 2D spectrum. Fringe frames were created by clipping deviant pixels (including pixels with flux from objects) and by averaging the unclipped pixels. Since the intensity of rows (the spatial axis of the spectra are along detector rows) can vary with respect to one another, each row is treated individually. The fringe frames were subtracted from the data after suitable scaling. Again, each row was treated individually. To help locate cosmic rays, an average sky spectrum was added back to the 2-dimensional fringe-corrected data. These data were then registered and combined, after clipping for cosmic rays, and a spectrum of the candidate extracted.

2.4. Spectral Fitting Method and SN Type Classification

We determine SN types by fitting spectra with spectral templates using software developed by Tokita (2009). The software fits the spectra over a grid of parameters: redshift, supernova template, extinction, and, if necessary, the host galaxy template and the fraction of host galaxy light. The templates consist of observed spectra of all SN types available from the literature, the FOCAS spectra of SDSS SNe (Zheng et al. 2008; Tokita 2009; K. Konishi in preparation), and synthetic spectra of SN Ia (Hsiao et al. 2007) and the other non-Ia types (Nugent et al. 2002). The software computes the reduced χ^2 and determines the best combination of type, redshift, extinction, and epoch of each SN for which the reduced χ^2 value is smallest. The extinction law used in this paper was from Cardelli, Clayton, and Mathis (1989). We also considered host

[2] For the Subaru 2001 Campaign a detector mosaic of two 2k × 4k 3-side buttable CCDs fabricated by SITe were used. For all other campaigns, a mosaic of MIT/LL CCDs were used.

[3] IRAF is distributed by the National Optical Astronomy Observatories, which are operated by the Association of Universities for Research in Astronomy, Inc., under cooperative agreement with the National Science Foundation.

Table 2. Summary of FOCAS Observations.*

Program	Date (UT)	Exposure	Targets	Mode	Configuration	Standard Star
S01A-079	2001/05/26	600 × 1	SDF1	LS	300B/SY47	Feige 34
(2)		2100 × 3	SDF5	LS	300B/SY47	Feige 34
	2001/05/27	900 × 1	CL1604_0-1	LS	300B/SY47	Feige 34
		2100 × 2	1520.1-2	LS	300B/SY47	Feige 34
		2100 × 3	SDF2	LS	300B/SY47	Feige 34
		2100 × 1	SDF4	LS	300B/SY47	Feige 34
		900 × 1	SDF6	LS	300B/SY47	Feige 34
S02A-174	2002/04/17	1800 × 3	S02-032	LS	300B/SY47	Feige 34
(1)		1500 × 1	C02-005	LS	300B/SY47	Feige 34
		1800 × 1	C02-007	LS	300B/SY47	Feige 34
S02B-I04	2002/11/13	2400 × 3	SuF02-012	LS	300R/SO58	Feige 110
(2)		1800 × 3	SuF02-061	LS	300R/SO58	Feige 110
S05B-137	2005/09/26	1800 × 5	SCP05D0	LS	300R/SO58	LTT 2415
(1.5)		1800 × 3	SCP05P1	LS	300R/SO58	LTT 2415
	2005/09/27	1800 × 2	SCP06N10	LS	300R/SO58	GD 71
	2005/09/28	1800 × 6	SCP05D6	LS	300R/SO58	GD 71
S05B-137	2005/10/26	1800 × (4+2)†	SCP05D6	LS	300R/SO58	BD + 28 4211
(1.5)		1800 × 3	SCP05P9	LS	300R/SO58	BD + 28 4211
	2005/10/27	1800 × 4	SCP05D6	LS	300R/SO58	BD + 28 4211
		1800 × 4	SCP05P9	LS	300R/SO58	BD + 28 4211
	2005/10/28	1800 × 2	SCP06X13	LS	300R/SO58	GD 71
S05B-137 (0.5)	2005/12/27	1800 × 4	SCP06X18	LS‡	300R/SO58	Feige 34
S05B-137	2006/04/22	1200 × 5	SCP06F3, SCP06F6, SCP06F8	F_mask2B	300R/SO58	Feige 34
(3)	2006/04/23	1200 × 5	SCP06X26, SCP06X27	X_mask1	300R/SO58	Feige 34
		1200 × 5	SCP06H3	H_mask2	300R/SO58	Feige 34
		1200 × 9	SCP06G3, SCP06G4	G_mask1	300R/SO58	Wolf 1346
		1200 × 2	SCP06F3, SCP06F6, SCP06F8	F_mask2B	300R/SO58	Hz 44
	2006/04/24	1200 × 2	SCP06X26, SCP06X27	X_mask1	300R/SO58	Feige 34
		1200 × 10	SCP06G3, SCP06G4	G_mask1	300R/SO58	Wolf 1346
S05B-137	2006/06/28	1200 × 4	SCP06F6, SCP06F12	F_mask2B	300B/SY47	Wolf 1346
(1.5)		1200 × 2	SCP06L22	LS	300B/SY47	Hz 44
	2006/06/29	1200 × 8	SCP06A4	A_mask1	300R/SO58	BD + 28 4211
		1200 × 9	SCP06K0, SCP06K18	K_mask1	300R/SO58	Hz 44
S06B-085	2006/08/23	1200 × 2	SCP06F6	LS	300B/SY47	Wolf 1346
(1)		1200 × 6	SCP06B3, SCP06B4	B_mask1B	300R/SO58	Wolf 1346
		1200 × 3	SCP06V6	V_mask1	300R/SO58	G 191-B2B
		1200 × 6	SCP06N32, SCP06N33	N_mask1	300R/SO58	G 191-B2B
S06B-085	2006/12/24	1200 × 8	SCP05D0, SCP05D6	D_mask1	300R/SO58	BD + 28 4211
(1)		1200 × 6	SCP05D0, SCP05D6	D_mask2	300R/SO58	BD + 28 4211
		1200 × 8	SCP06X18, SCP06X26, SCP06X27	X_mask2	300R/SO58	Feige 34
		1200 × 4	SCP06E12	E_mask3	300R/SO58	Feige 34
S06B-085	2007/05/18	1200 × 6	SCP06E12	E_mask4	300R/SO58	Hz 44
(2)		1200 × 6	SCP06T1	T_mask1	300R/SO58	BD + 28 4211
	2007/05/19	1200 × 7	SCP06E12	E_mask6	300R/SO58	Hz 44
		1200 × 7	SCP06T1	T_mask2	300R/SO58	BD + 28 4211

* Column 1 denotes observing programs for FOCAS observations and allocated nights in parentheses. Column 2 denotes observing dates in yyyy/mm/dd. Exposure times (in seconds), target names, spectroscopic modes, grism/order-sort filter configurations, and standard stars used for flux calibration are listed in columns 3, 4, 5, 6, and 7. The letters "LS" indicate that the long-slit mode was used. When the multi-object spectroscopic mode was used, the slitmask name is used instead. The spectroscopic configuration was either 300B/SY47 or 300R/SO58, which provide spectra over the 4700–9000Å and 5800–10000Å wavelength ranges, respectively. In addition to the night listed below, 6 nights were lost to clouds.

† SCP05P9 was observed between the two exposures positions.

‡ Slit positioning may have failed as there was no signal.

Table 3. Summary of FOCAS spectrum fitting results.[†]

Name 1	Name 2	$z_{\rm gal}$	$z_{\rm SN}$	Template	$t_{\rm sp}$	$t_{\rm LC}$[‡]	C.I.[§]	Type[§]	Notes
CL1604_0-1	SN 2001cq	—	0.36	SN 1998aq	−8	—	5	Ia	Si II, S II.
1520.1-2	SN 2001cw	0.94	0.95	Hsiao Ia	−6	−5	3	Ia*	4000Å break.
SDF1	SN 2001cs	0.431	0.42	SN 1994D	−1	—	5	Ia	Ca II H and K. Sig. host galaxy contamination.
SDF2	SN 2001ct	—	?	—	—	—	1	II?	Blue continuum.
SDF4	SN 2001cr	—	?	—	—	—	2	?	—
SDF5	SN 2001cv	1.039	1.02	Nugent Ia	20	—	2	?	[O II][#].
SDF6	SN 2001cu	0.515	0.50	Nugent Ib/c	−6	—	2	?	Ca II H and K. Sig. host galaxy contamination.
			0.50	Hsiao Ia	−6				Sig. host galaxy contamination.
S02-032	SN 2002ff	—	1.02	Nugent Ia	0	0	4	Ia	—
C02-005	—	0.426	—	—	—	—	0	SB/AGN	Starburst or AGN.
C02-007	—	1.780	—	—	—	—	0	AGN	AGN.
SuF02-012	SN 2002lc	—	1.22?	—	—	−1	2	?	Sig. host galaxy contamination.
SuF02-061	—	1.085	—	—	—	∼5	2	?	Sig. host galaxy contamination. AGN?
SCP06A4	Aki	1.19	—	—	—	0	2	?	Low signal-to-noise ratio.
SCP06B3	Isabella	0.744	—	—	—	13	2	?	[O II], Hβ, [O III].
SCP06B4	Michaela	1.117	—	—	—	4	2	?	[O II], [Ne III].
SCP05D0	Frida	1.015	—	—	—	16	—	—	Ca II H and K.
			—	—	—	241	—	—	Ca II H and K. Table 4.
SCP05D6	Maggie	1.315	—	—	—	−8	2	?	Ca II H and K.
			—	—	—	4	2	?	Ca II H and K.
			—	—	—	187	—	—	Ca II H and K. Table 4.
SCP06E12	—	—	—	—	—	>300	—	—	Nearby galaxy at $z = 1.025$.
			—	—	—	>480	—	—	—
SCP06F3	—	1.21?	—	—	—	0	2	?	An emission line at 6195Å? AGN?
SCP06F6	—	—	—	—	—	−25	0	non-Ia	Blue continuum. Barbary et al. 2009.
			—	—	—	42	0	—	Weak continuum.
			—	—	—	98	0	—	Very low signal-to-noise ratio.
SCP06F8	Ayako	0.789?	—	—	—	40	—	—	Spectrum dominated by the neighbor.
SCP06F12	Caleb	—	—	—	—	194	—	—	Almost no continuum.
SCP06G3	Brian	0.962	—	—	—	24	—	—	[O II][#].
SCP06G4	Shaya	1.350	1.35	Hsiao Ia	−1	−5	3	Ia*	Probable Ca II H and K. Table 4.
SCP06H3	Elizabeth	0.851	0.84	Hsiao Ia	2	0	4	Ia	[O II], [O III].
SCP06K0	Tomo	1.416	—	—	—	68	—	—	4000Å break. Table 4.
SCP06K18	—	1.411	—	—	—	84	—	—	4000Å break. Table 4.
SCP06L22	—	1.369	—	—	—	—	0	AGN	broad Mg II.
SCP06N10[‖]	—	0.203	—	—	—	>54	—	—	[O III], Hα.
SCP06N32	—	—	—	—	—	<3	2	Ib/c?	—
SCP06N33	Naima	1.189	—	—	—	4	2	?	Very low signal-to-noise ratio.
SCP05P1	Gabe	0.926	—	—	—	16	—	—	[O II], [O III].
SCP05P9	Lauren	0.821	0.81	Hsiao Ia	−2	−3	3	Ia*	Sig. host galaxy contamination. [O II], [O III], Hβ.
SCP06T1	Jane	1.112?	—	—	—	450	—	—	Probable [O II].
SCP06V6	—	0.903	—	—	—	—	0	AGN	[O II], Fe II, broad Hβ, [O III].
SCP06X13	—	1.642	—	—	—	—	0	AGN	Broad Mg II.
SCP06X18	—	—	—	—	—	16	2	?	Almost no continuum.
			—	—	—	378	—	—	Almost no continuum.
SCP06X26	Joe	1.44?	—	—	—	67	—	—	A marginal emission line at 9100Å.
			—	—	—	312	—	—	—
SCP06X27	Olivia	0.435	—	—	—	38	—	—	Na I D, Hα, [N II].
			—	—	—	208	—	—	Na I D, Hα, [N II].

[†] Columns 1 and 2 are target names. In column 2, we list the IAU name, if the SN was reported in an IAU circular. Otherwise, this field is either left blank or is filled with the nicknames of the candidates. Columns 3 and 4 are the redshifts from the host galaxies and SNe. If we could classify a candidate as a SN, we report the name and epoch of the best-fitting local SN in columns 5 and 6, respectively. Epochs from the light curve fits are denoted in column 7. The confidence index (C.I.) of the classification and the object type are listed in columns 8 and 9, respectively. Notes on individual objects are in column 10.

[‡] In rest frame days, except for SCP06F6, SCP06E12, SCP06F3, SCP06F8, SCP06F12, SCP06N32, SCP06T1, SCP06X18, and SCP06X26, which are in observer frame days.

[§] Generally left as "—" for targets that were observed more than two rest frame weeks after maximum light, where the host galaxy was the primary target.

[‖] No fringe corrections were applied. A 1.″0-width slit was used.

[#] The single emission line is identified as [O II].

galaxy contamination in some cases. Errors in the template spectrum were neglected.

When the redshift of the host, $z_{\rm gal}$, could be determined from host galaxy spectral features, we allowed the redshift of the SN, $z_{\rm SN}$, to be fitted in the range $\Delta z \equiv |(z_{\rm gal} - z_{\rm SN})| \sim \pm$ 0.01–0.02. The range allowed for velocity variations found in normal SNe and, to a much smaller degree, a velocity offset due to the motion of the SN with respect to the host. When the light curve could be well-fitted by light curve templates, differences between the epochs, Δt, were expected to be within $\sim \pm 3$ days. We note that epochs of spectra t and τ were defined as days from the maximum light and explosion, respectively, and that t was generally applied for SNe Ia, while τ was applied for core-collapse SNe. Larger differences of epochs were possible for later phases because the number of SN spectral templates that were available was not so large. For most of SN candidates discovered during the Subaru 2001 and Spring 2002 campaigns, there were too few light-curve epochs to set strong constraints on the spectroscopic epoch.

In some cases, the extracted SN spectrum was contaminated by host-galaxy light. If the contamination was significant, we removed the host-galaxy light using one of two methods. In the case that the SN and the host galaxy were well resolved, we subtracted a spectrum that was extracted from a region located on the other side of the center of the host. We assumed axial symmetry of the host galaxy. When the SN was located close to the center of the host galaxy, we subtracted a synthetic spectrum computed from the spectral library of Bruzual and Charlot (2003) (hereafter BC03). In the second case, the amount of host contamination was estimated by minimizing the reduced χ^2. When the SN was almost free from contamination of the host galaxy, judged from a visual inspection of the imaging and spectroscopic data, we did not make any corrections for the host galaxy.

We quantified the degree of confidence that we had correctly classified a candidate as a SN Ia using the index described in Howell et al. (2005). A confidence index (C.I.), ranging from 5 to 0, was assigned to each SN candidate that was observed within two rest-frame weeks of the maximum light. In addition to the spectra, information from the lightcurve and the host, if available, were used to set this index. Candidates with 5, 4, 3, 2, 1, and 0 were *certain SN Ia*, *highly probable SN Ia*, *probable SN Ia*, *unknown object*, *probably not a SN Ia*, and *not a SN Ia*, respectively. For those candidates that were classified as SNe Ia with C.I. of 5, 4, and 3, we list the best matching template in table 3 and plot the candidate and the best matching template in the figures of the following section. We also made this comparison for selected candidates with C.I. of 2. Following Howell et al. (2005), SNe Ia, which was assigned a C.I. of 4 or 5 were typed as SN Ia, and those that were assigned a C.I. of 3 were typed as SN Ia*, which indicates a higher degree of uncertainty for these SNe. No classification was made for the candidates that were observed more than two weeks after the maximum light, where the host galaxy was the primary target.

As a cross check of the classification, all spectra were fitted with *superfit* (Howell et al. 2005) and independently classified by two of the authors. In nearly all cases, the classifications matched. For those few cases in which there was some disagreement, always small, we usually adopted the more conservative classification.

The fitting results are summarized in table 3.

3. SN Type Classification Results

In the following sections, we show spectra of 8 candidates from the Subaru 2001 and Spring 2002 search campaigns, 2 spectra from the Fall 2002 search campaign in the SXDS fields, and 10 spectra from the HST Cluster Supernova Survey. The confidence in the spectral classifications varies from 5, a secure SNe Ia (SDF1, for example), to 0, not a SN Ia (SCP06F6, for example). The spectra of candidates that are clear AGN (C02-007 and SCP06V6, for example) are not shown. Also, the FOCAS spectrum of the extraordinary transient SCP06F6 was presented in Barbary et al. (2009), and is not re-shown here. All of the candidates observed with FOCAS are summarised in tables 2 and 3.

For display purposes only, the spectra shown in the following figures were smoothed with a Gaussian (FWHM of $\sim$30 pixels or $\sim$40 Å) with each point weighted with the inverse of its variance. Although telluric absorption features were removed using the spectra of bright stars, the correction was not perfect, so these regions are highlighted in gray. Also highlighted are residuals from the strong atmospheric emission lines, such as those from Oxygen (5577 Å and 6300 Å) and Sodium (5890 Å). Non-stellar features, such as the [O II] emission line, which are not reproduced by BC03 models, are also marked. These regions can bias spectral fitting results, so they are masked out. The Suprime-Cam and ACS finding charts are $8'' \times 8''$and $5'' \times 5''$, respectively. North is up and East is to the left.

3.1. Candidates from the Subaru Spring Searches

All of the SN candidates shown in this section were found with Subaru Suprime-Cam in the springs of 2001 and 2002.

3.1.1. CL1604_0-1

CL1604_0-1 (SN 2001cq) was found in the field surrounding the galaxy cluster CL1604. On 2001 May 27, we obtained a spectrum with an exposure of 900 s. The host galaxy could not be detected in the images. The spectrum (figure 1) does not show any significant spectral features from the host galaxy and $z_{\rm gal}$ could not be determined. Clear Si II 4000Å, S II "w", and Si II 6150Å features were detected, indicating that this is a secure SN Ia at $z_{\rm SN} = 0.36$. The C.I. is 5. The best-fit SN spectrum is a normal SN Ia, SN 1998aq, at $t = -8$ days.

3.1.2. 1520.1-2

1520.1-2 (SN 2001cw) was found in the field centered on the galaxy cluster 1520.1. The FOCAS spectrum (figure 2) was obtained on 2001 May 27, and the exposure was 4200 s. The SN is well separated from the probable host, which is located to the northeast of the SN. The redshift of this galaxy is $z_{\rm gal} \sim 0.94$, as determined from the 4000Å break. The spectrum could fitted with both the Nugent Type Ib/c template at $t = -4$ days redshifted to $z_{\rm SN} = 0.95$ and the Hsiao Type Ia template at $t = -6$ days redshifted to $z_{\rm SN} = 0.95$. The light curve is consistent with that of a SN Ia (R. Amanullah et al., in preparation) and also $t_{\rm sp}$ matches $t_{\rm LC}$. We conclude that it is a probable SN Ia and set the C.I. to 3.

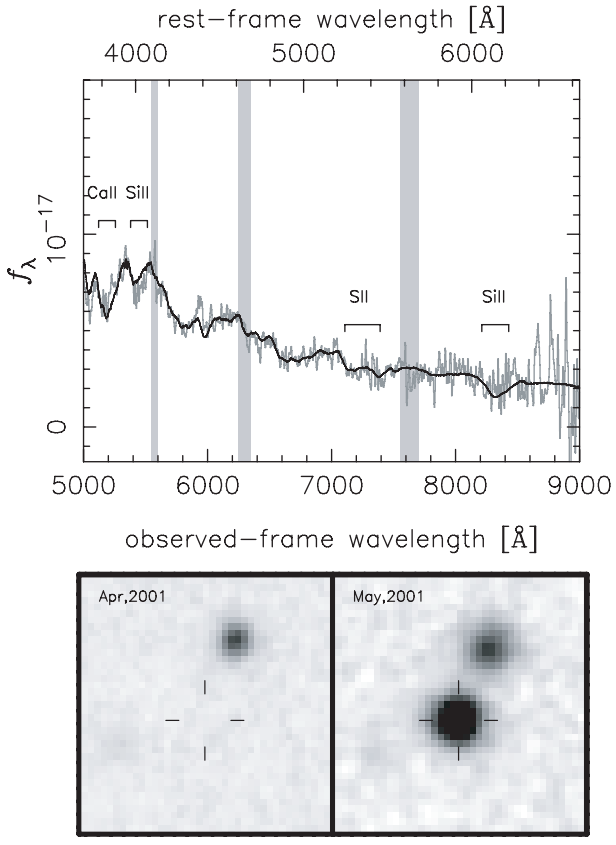

Fig. 1. (Top): Spectrum of CL1604_0-1 (SN 2001cq) at $z_{\rm SN} = 0.36$ (gray) and the redshifted spectrum of SN 1998aq at $t = -8$ day (black). The host galaxy redshift $z_{\rm gal}$ can not be determined. Light-gray regions are masked because of atmospheric absorption or missubtraction of the sky background. The C.I. is 5. (Bottom): Finding charts of CL1604_0-1. The size is $8'' \times 8''$. North is up and east is left.

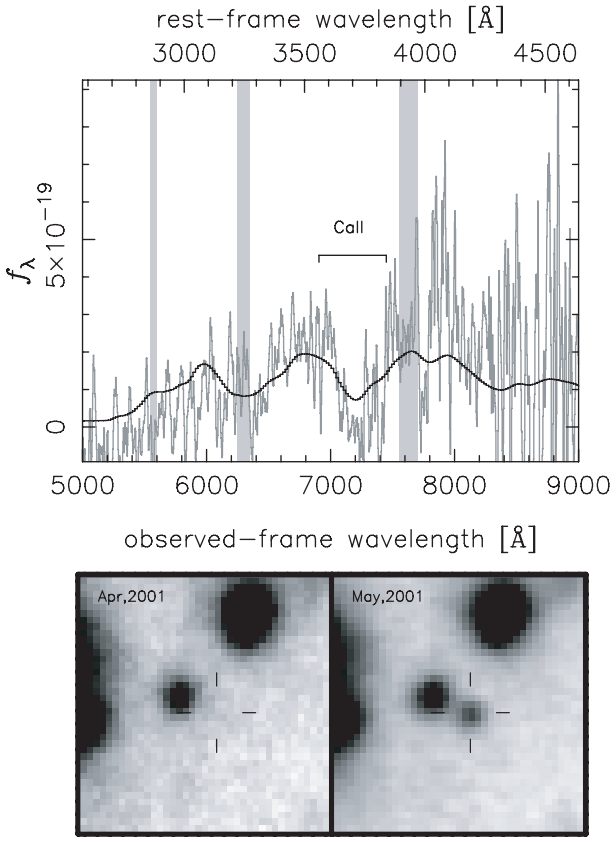

Fig. 2. (Top): Spectrum of 1520.1-2 at $z_{\rm gal} \sim 0.94$ (gray) and the Hsiao Ia template at $t = -6$ days (black) redshifted to $z_{\rm SN} = 0.95$. The C.I. is 3. (Bottom): Finding charts of 1520.1-2.

3.1.3. SDF1

SDF1 (SN 2001cs) was found during the 2001 run of the SDF project together with other SDF SN candidates (SDF2, SDF4, SDF5, and SDF6). This SN is only slightly offset from the center of the relatively bright host. Not surprisingly, the SN spectrum is strongly contaminated by host galaxy light. The 600 second spectrum (figure 3) taken on 2001 May 26 indicates that the host galaxy is at $z_{\rm gal} = 0.431$ from Ca II H and K absorption lines. After subtracting a model of the host galaxy spectrum and correcting for extinction [$E(B-V) = 0.2$ mag], the distinctive Si II feature of SNe Ia around 4000Å in the rest frame could be seen. This is a SN Ia with the C.I. of 5 at $z_{\rm SN} = 0.42$. The best-fit spectrum is SN 1994D at $t = -1$ day.

3.1.4. SDF2

The spectrum of SDF2 (SN 2001ct) is shown in figure 4. It was taken on 2001 May 27, and has a total integration time of 6300 s. This SN appears on a diffuse galaxy. The redshift of the likely host could not be determined, and the spectrum of the SN is featureless and blue. We could determine neither the type nor the redshift of SDF2; however, the blue continuum suggests that this candidate is probably a Type II SNe. The C.I. is 1.

3.1.5. SDF4

The spectrum of the unusual transient SDF4 (SN 2001cr) is shown in figure 5. It was taken on 2001 May 27, and had a total integration of 2100 s. The Suprime-Cam reference image taken in 2002 April does not show any significant signal from the either the SN or the host. The SN component dominates the spectrum. The redshift of the host galaxy, $z_{\rm gal}$, could not be determined. There are no SN templates that fit the observed spectrum well. The best-fit SN template is the Nugent SN Ib/c hypernova (HN) template at $t = 0$ days redshifted $z_{\rm SN} = 0.78$. But some bumpy structures in the spectrum do not match well. A SN 1991T template at $t = -11$ days redshifted to $z_{\rm SN} = 0.81$ might fit the spectrum better, although the χ^2 values are slightly larger. The C.I. is 2.

3.1.6. SDF5

The spectrum of SDF5 (SN 2001cv) is shown in figure 6. It was taken on 2001 May 26 and has a total integration of 5300 s. The SN is separated from the host galaxy and the SN component dominates the spectrum at the location of the SN. The redshift of the host is $z_{\rm gal} = 1.039$, as measured from a single strong emission line, which we identified as [O II]. It is very unlikley that the line is Lyα, as the line is not asymmetric, and the continuum across the line shows no evidence for a discontinuity. It is unlikely to be Hα or [O III], since no other lines are seen, despite the strength of the detected line. When the spectral template of a star forming galaxy was subtracted, the SN spectral fitting indicated that the Hsiao template SN Ia at $t = 9$ days at $z_{\rm SN} = 1.02$ is the best match. However, the spectral features characteristic of a SN Ia are marginal, and we

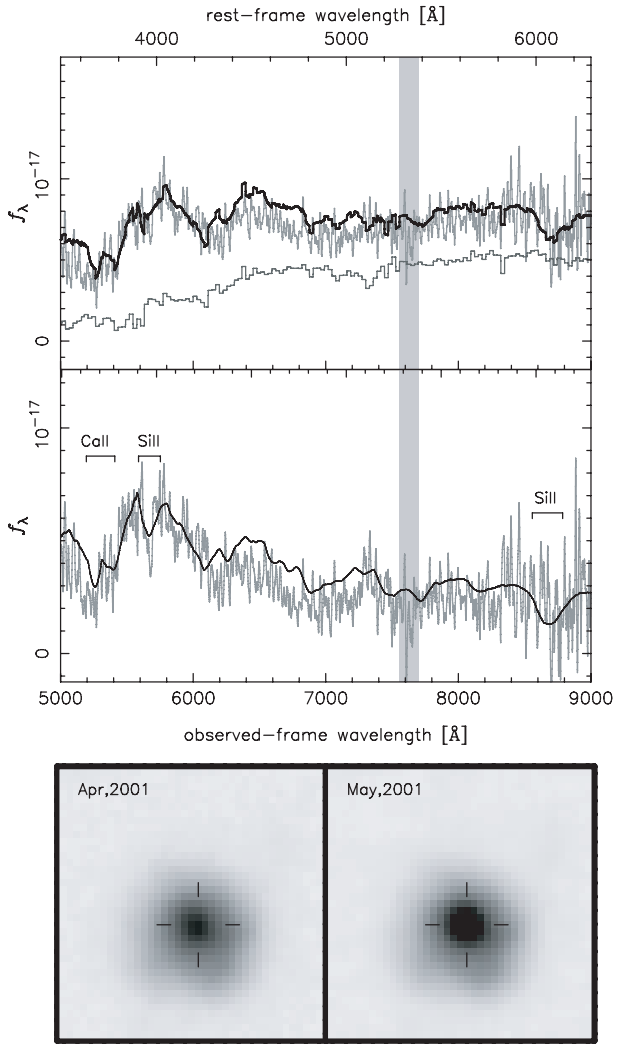

Fig. 3. (Top): In the upper panel, the spectrum of SDF1 (SN 2001cs) at $z_{\rm gal} = 0.431$ (gray), the galaxy template subtracted spectrum (dark gray), and the combined SN template plus galaxy template spectrum (black). In the lower panel, the galaxy-subtracted spectrum (gray) and and the spectrum of the best matching local SN, SN 1994D at $t = -1$ days, redshifted to $z_{\rm SN} = 0.42$ (black). The C.I. is 5. (Bottom): Finding charts of SDF1.

could not obtain a well-sampled light curve. Therefore, we set the C.I. to 2.

3.1.7. SDF6

The spectrum of SDF6 (SN 2001cu) is shown in figure 7. It was taken on 2001 May 27, and has a total integration time of 900 s. The host is similar in brightness to the SN, so the SN spectrum is contaminated by light from the host. A redshift of $z_{\rm gal} = 0.515$ was measured from the Ca II H and K absorption lines of the host galaxy. After subtracting a passively evolving model for the spectrum of the host galaxy and correcting for extinction [$E(B-V) = 0.2$ mag], both the Nugent Ib/c template at $t = -6$ days redshifted to $z_{\rm SN} = 0.50$ and the Hsiao Ia template at $t = -6$ days redshifted to $z_{\rm SN} = 0.50$ were acceptable fits to the spectrum. Since there are too few light curve points to help with the classification, C.I. was set to 2.

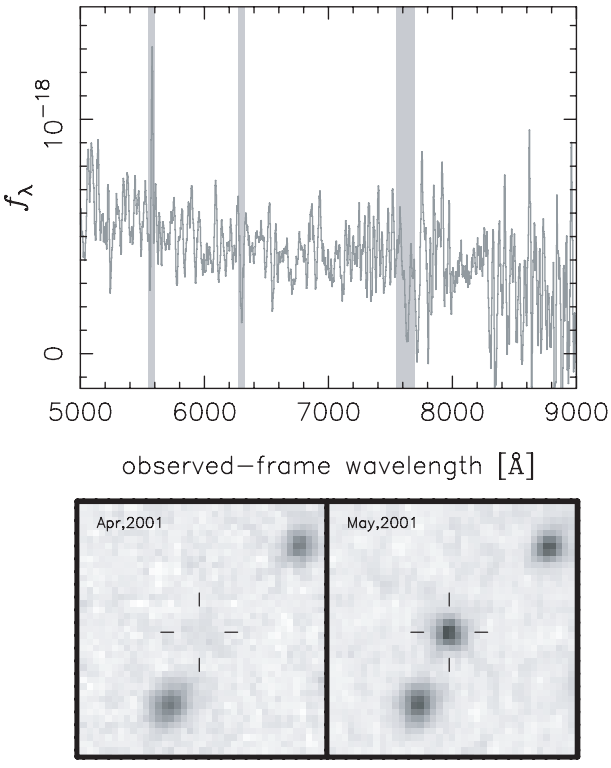

Fig. 4. (Top): Spectrum of SDF2 (SN 2001ct). The C.I. is 1. (Bottom): Finding charts of SDF2.

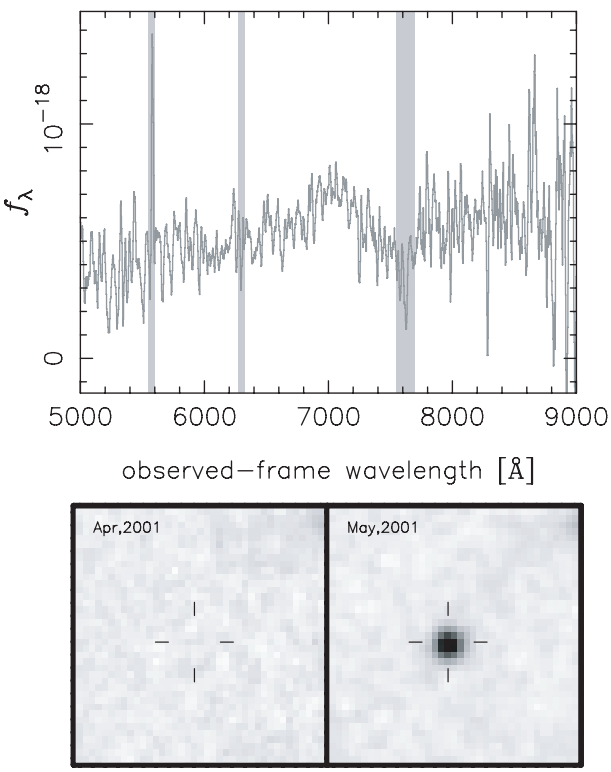

Fig. 5. (Top): Spectrum of SDF4 (SN 2001cr). The C.I. is 2. (Bottom): Finding charts of SDF4.

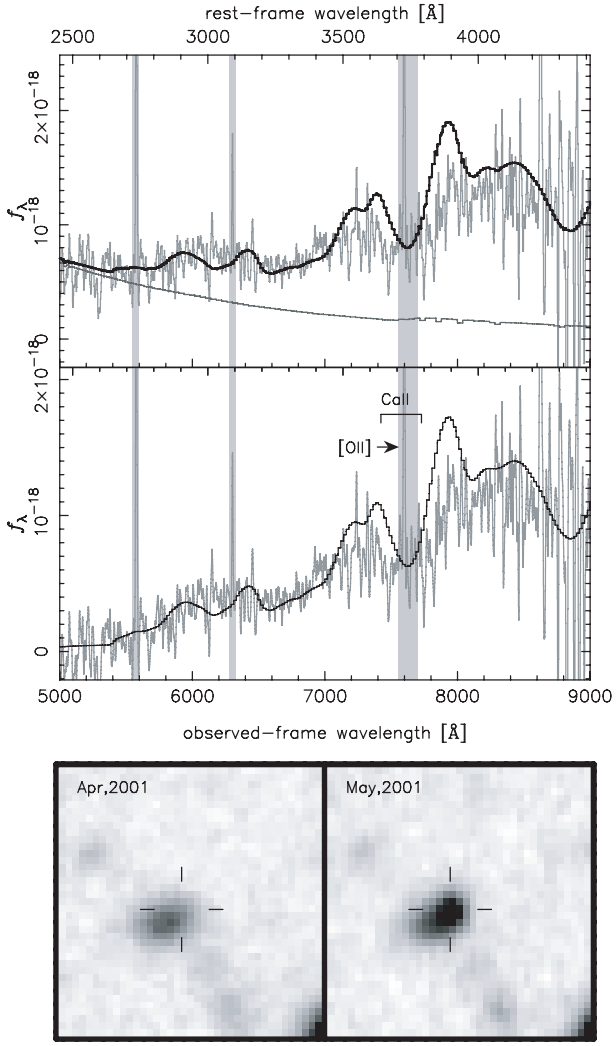

Fig. 6. (Top): Spectrum of SDF5 (SN 2001cv) at $z_{\rm gal} = 1.039$ (gray) and the Hsiao SN Ia template at $t = 9$ days redshifted to $z_{\rm SN} = 1.02$ (black). The C.I. is 2. (Bottom): Finding charts of SDF5.

3.1.8. S02-032

The spectrum of S02-032 (SN 2002ff) is shown in figure 8. It was taken on 2002 April 17, and had a total integration time of 5400 s. This SN appears on a diffuse galaxy whose redshift could not be measured. The SN component dominates the spectrum. The SN spectral fitting indicates that this is a SN Ia at $z_{\rm SN} = 1.02$. The best-fit spectrum template is the Nugent normal Ia template at $t = 0$ days. The light curve is consistent with that of a SN Ia and $t_{\rm sp}$ matches $t_{\rm LC}$. C.I. is 4.

3.2. Candidates in the SXDS Field

All of the SN candidates shown in this section were found with Subaru Suprime-Cam during an SN campaign conducted during the Fall of 2002.

3.2.1. SuF02-012

The spectrum of SuF02-012 (SN 2002lc) is shown in figure 9. It was observed on 2002 November 13, and had a total integration time of 7200 s. It is hosted by a diffuse galaxy, whose redshift could not be determined. The spectral fitting

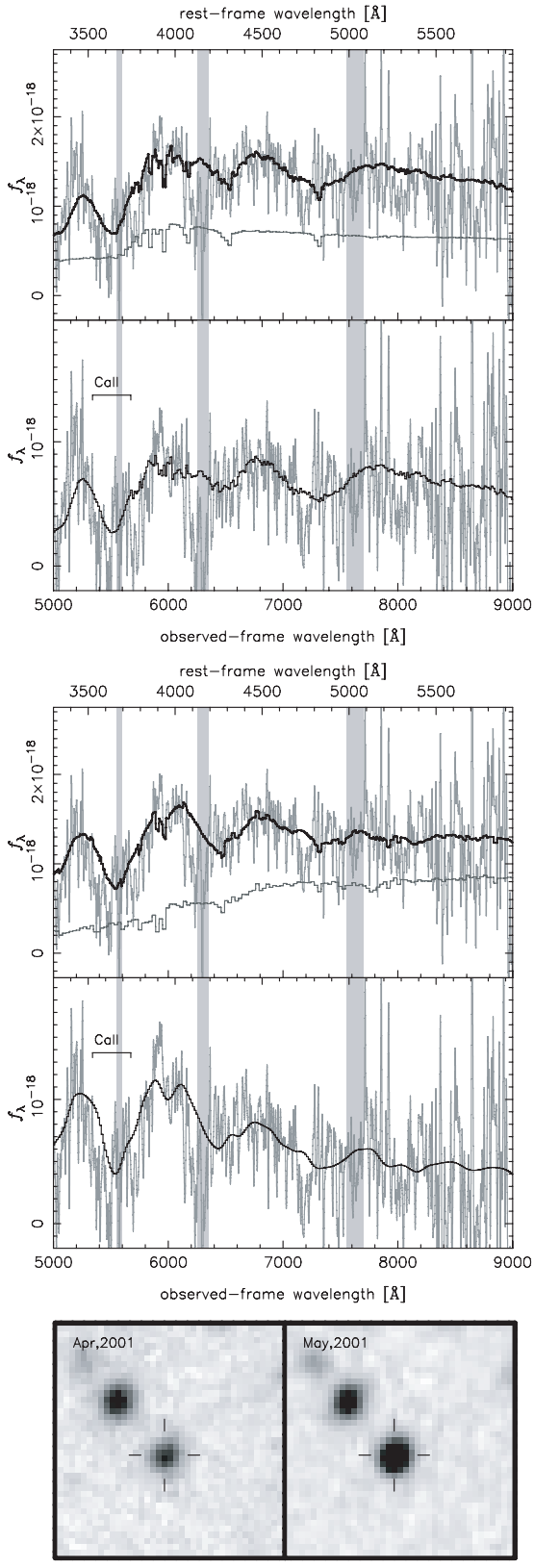

Fig. 7. (Top): Spectrum of SDF6 (SN 2001cu) at $z_{\rm gal} = 0.515$ (gray) and the Nugent Ib/c template at $t = -6$ days redshifted to $z_{\rm SN} = 0.50$ (black). (Middle): Spectrum of SDF6 at $z_{\rm gal} = 0.515$ (gray) and the Hsiao Ia template at $t = -6$ days redshifted to $z_{\rm SN} = 0.50$ (black). The C.I. is 2. (Bottom): Finding charts of SDF6.

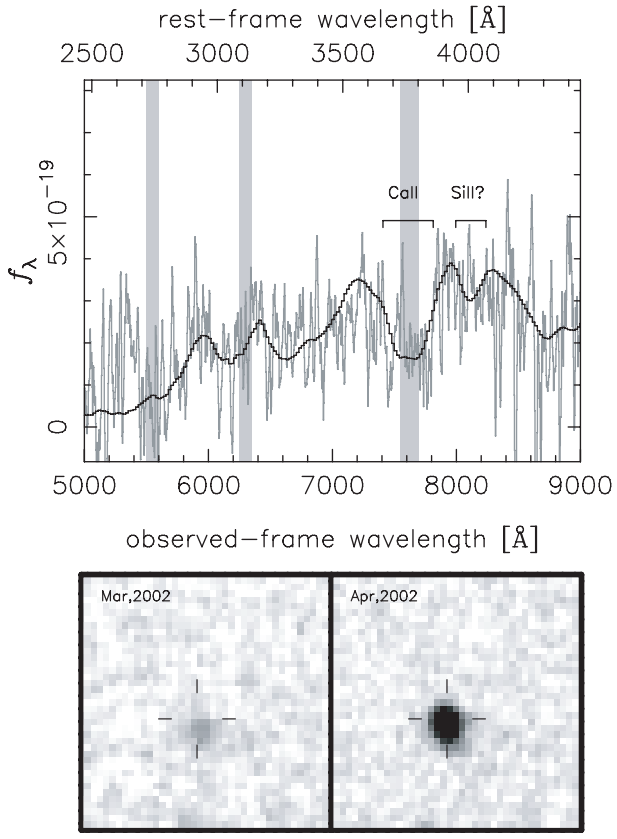

Fig. 8. (Top): Spectrum of S02-032 (SN 2002ff) at $z_{\rm SN} = 1.02$ (gray) and the Nugent Ia template at $t = 0$ days (black) redshifted to $z_{\rm SN} = 1.02$. The C.I. is 4. (Bottom): Finding charts of S02-032.

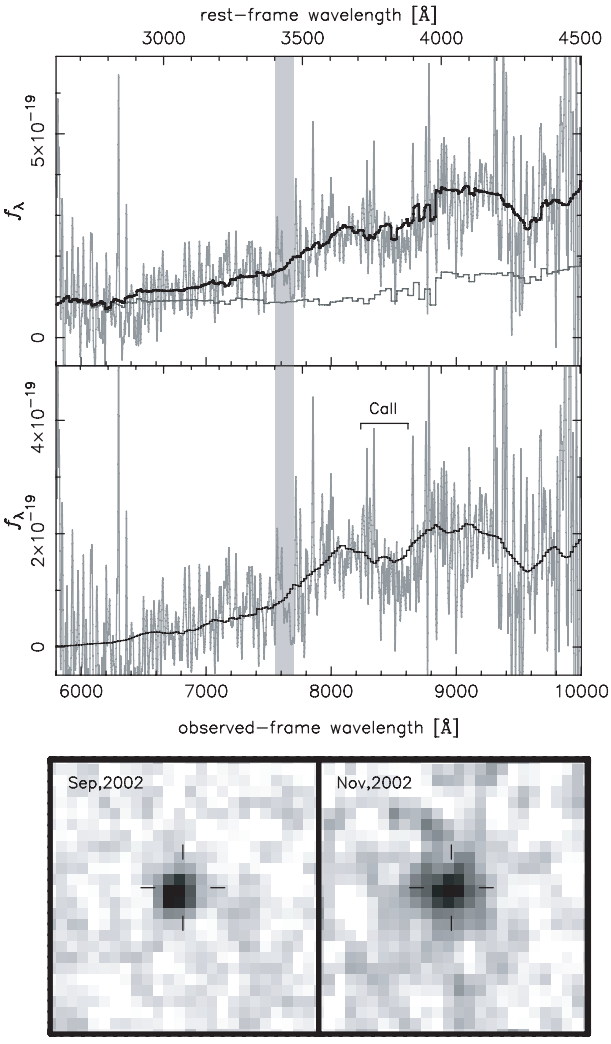

Fig. 9. (top): Spectra of SuF02-012 (SN 2002lc) at $z_{\rm SN} = 1.22$ (gray) and SN 1991T at $t = 12$ days (black) redshifted to $z_{\rm SN} = 1.22$. The C.I. is 2. (bottom): Finding charts of SuF02-012.

indicates that it might be a SN Ia at $z_{\rm SN} = 1.22$. However, the phase of the best-fit template, SN 1991T at $t = 12$ days, disagrees with the light-curve phase. SNe Ia at earlier phases and higher redshifts are also a possibility. Given the uncertainty, we set C.I. to 2. This target was a high-priority object, and spectroscopically observed with FORS2 on the ESO VLT, ESI on the Keck, and the ACS grism on the HST. All of the spectra suggest that this is a high-redshift SN. A future analysis of the combined data set may lead to this candidate being reclassified.

3.2.2. SuF02-061

The spectrum of SuF02-061 is shown in figure 10. It was taken on 2002 November 13 with a total exposure time of 5400 s. This SN appears on a diffuse galaxy that has a redshift of $z_{\rm gal} = 1.085$, as measured from several emission lines, including [O II], [Ne III], and some Balmer lines. The spectrum is too noisy, or the host light dominates too much to classify the SN type. This galaxy was also detected in X-rays, suggesting that the variability may originate from AGN activity. C.I. is 2.

3.3. Candidates from the HST Cluster Supernova Survey

All of the SN candidates shown in this section were found in the HST ACS survey for SNe Ia in distant galaxy clusters (HST Cluster Supernova Survey). On average, the SN candidates in this search are more distant than those found in earlier searches. Furthermore, since the survey aimed to find SNe Ia in early-type galaxies,[4] the relative brightness of such SN with respect to the host is usually small. Consequently, typing of these candidates generally needs to rely on other methods, such as the properties of the host. The principle aim of the spectroscopy is to obtain the redshift of the host. Note that the finding charts were made from images taken with ACS. They have greater spatial resolution than those made from images taken with Suprime-Cam, which were smoothed by the seeing.

3.3.1. SCP06B3

The spectrum of SCP06B3 is shown in figure 11. It was taken on 2006 August 22, and had a total integration time of 7200 s. A second candidate, SCP06B4 (sub-subsection 3.3.2), was observed in the same slitmask. SCP06B3 appears near to

[4] If a galaxy has no detectable star formation and has the morphology of an early type galaxy, then we use the term early-type to describe the galaxy. It is a definition that is commonly used throughout the literature. To our knowledge, there has never been a Type II Supernova in a galaxy where there was no detectable signs of star formation. Of course, some star formation may be beyond detection in our optical spectra because it is either heavily obscured or because the star formation rate is very low.

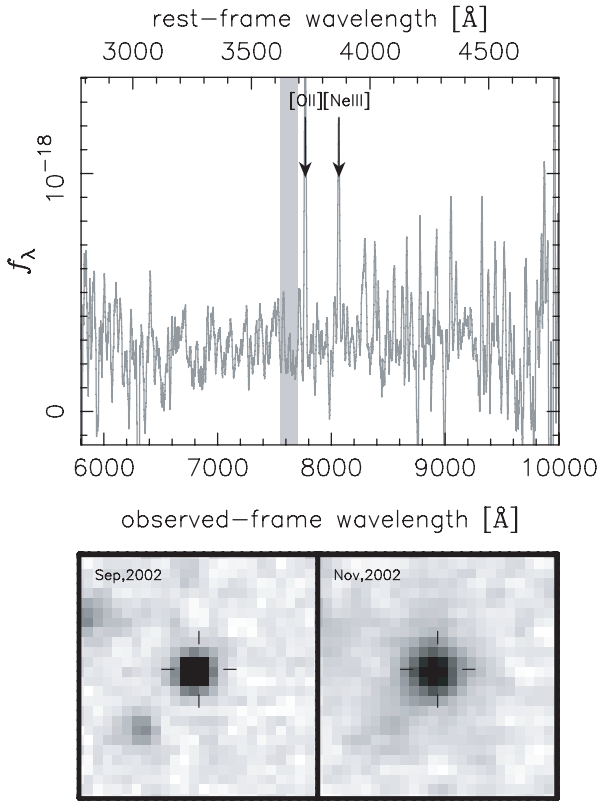

Fig. 10. (top): Spectra of SuF02-061 at $z_{\rm gal} = 1.085$. The C.I. is 1. (bottom): Finding charts of SuF02-061.

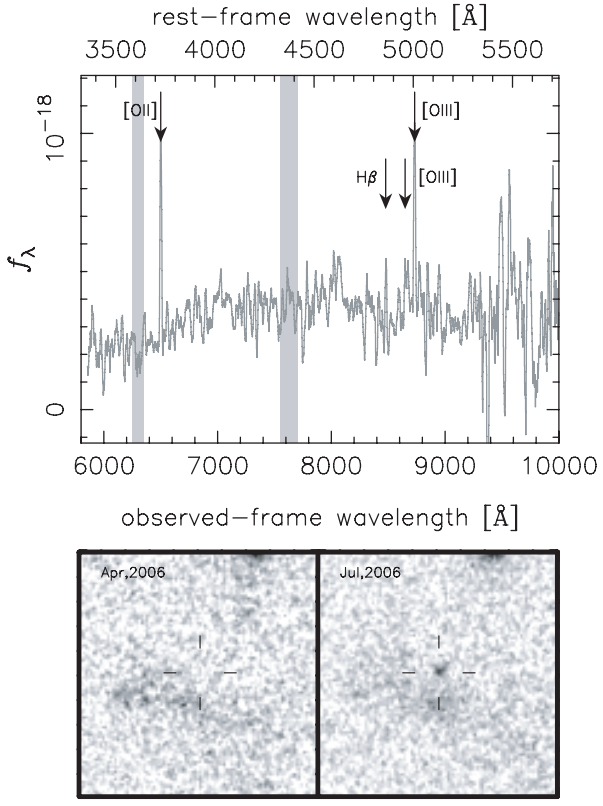

Fig. 11. (Top): Spectrum of SCP06B3 at $z_{\rm gal} = 0.744$ (gray). C.I. is 2. (Bottom): Finding charts of SCP06B3. The size is $5'' \times 5''$. North is up and east is left.

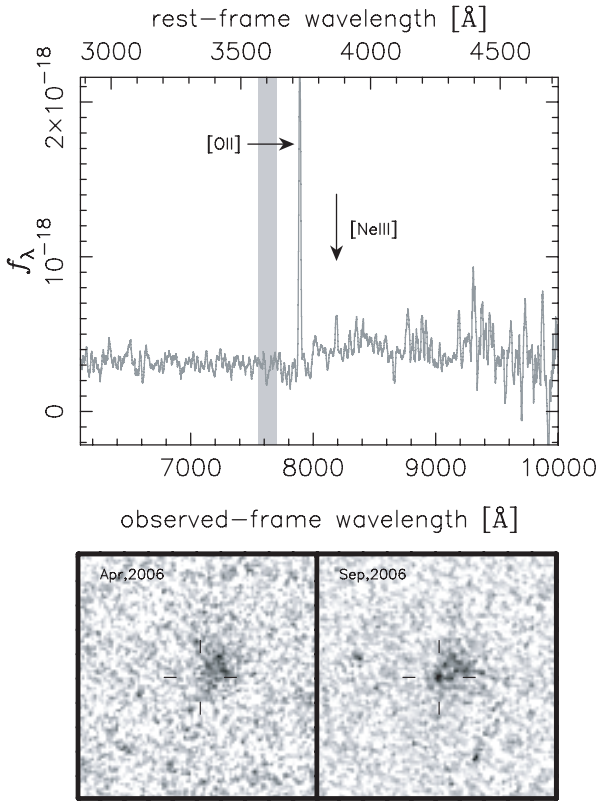

Fig. 12. (Top): Spectrum of SCP06B4 at $z_{\rm gal} = 1.117$ (gray). The C.I. is 2. (Bottom): Finding charts of SCP06B4.

a very diffuse galaxy that has a redshift of $z_{\rm gal} = 0.744$ from [O II], Hβ, and [O III] emission lines. The spectrum is dominated by host galaxy light, and a convincing type could not be obtained. C.I. is set to 2.

3.3.2. SCP06B4

The spectrum of SCP06B4 is shown in figure 12. It was taken on 2006 August 22, and had a total integration time of 7200 s. SCP06B4 appears near to a diffuse galaxy that has a redshift of $z_{\rm gal} = 1.117$, as measured from [O II] and [Ne III] emission lines. The spectrum of SCP06B4 appears to be dominated by light from the host. A convincing type for the transient could not be derived, so C.I. is set to 2.

3.3.3. SCP06F6

The extraordinary transient SCP06F6 was found on 2006 February 21. It shows a large (from below the detection limit in the ACS i_{775} and z_{850} bands) and slow ($\sim$ 5 months in the observer frame) increase in the flux (Dawson et al. 2006). For this interesting and unusual object, we took FOCAS spectra three times on 2006 April 22 (6000 s), 2006 June 28 (4800 s), and 2006 August 22 (2400 s). However, the signal-to-noise ratio of the last two spectra are too low to see any spectral features. SCP06F6 seems to be hostless. The properties of this object are discussed in detail in Barbary et al. (2009). It is quite unlike a SN Ia, so C.I. is set to 0.

3.3.4. SCP06G3

The spectrum of SCP06G3 is shown in figure 13. It was taken on 2006 April 23 and 24, and had a total exposure time of

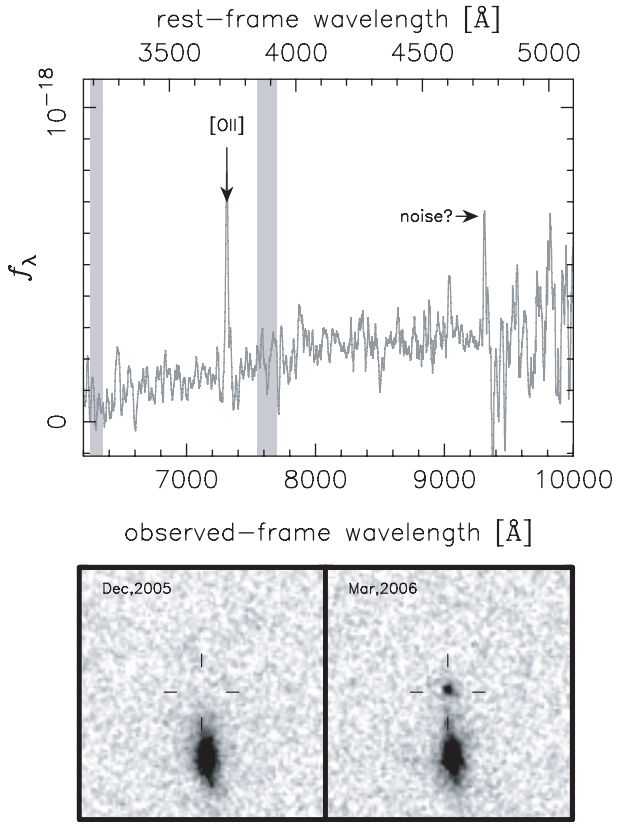

Fig. 13. (top): Spectrum of SCP06G3 at $z_{\rm gal} = 0.962$ (gray). The sharp feature at 9300Å is a noise artifact from the processing of the data and is not real. C.I. is 2. (bottom): Finding charts of SCP06G3.

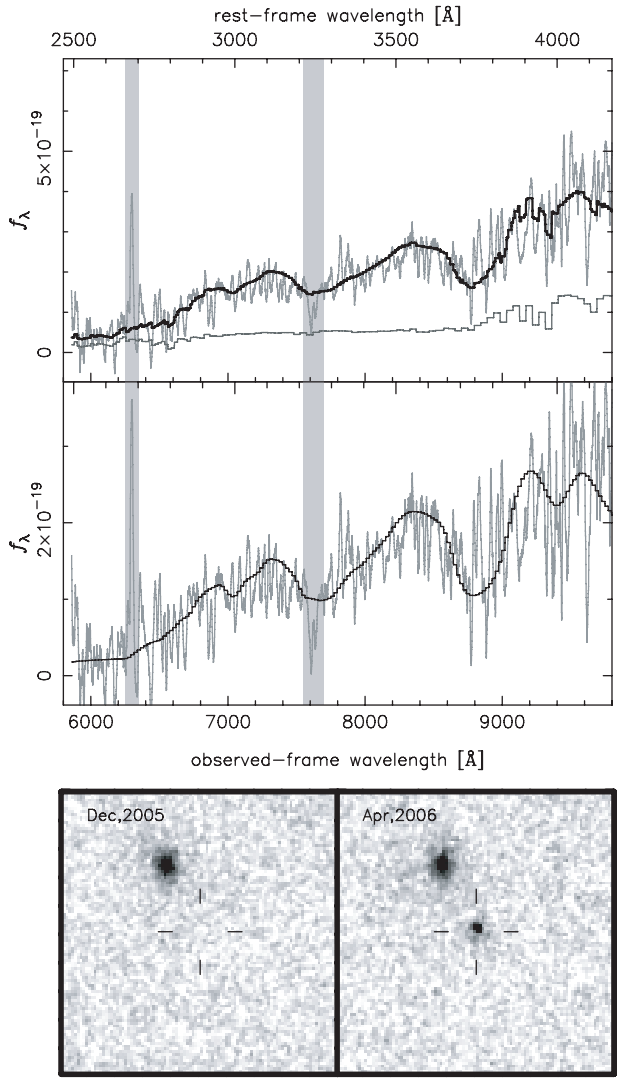

Fig. 14. (top): Spectrum of SCP06G4 at $z_{\rm gal,fit} = 1.350$ (gray) and the Hsiao Ia template at $t = -1$ day redshifted to $z_{\rm SN} = 1.35$ (black). The C.I. is 3. (bottom): Finding charts of SCP06G4.

22800 s. A second candidate, SCP06G4 (sub-subsection 3.3.5), was observed in the same slitmask. SCP06G3 appears to be associated with a galaxy that can be seen to the south of SCP06G3 (see figure 13). A single strong emission line, which we identified as [O II] from the host galaxy, led to a redshift of $z_{\rm gal} = 0.962$. Weak Balmer lines and a weak 4000Å break were also detected. The position angle of this slitmask was optimized for SCP06G4, which meant that the slit could not be set along the line joining SGP06G4 and the center of the host galaxy. Also, the spectrum was taken 24 days after the maximum light, so it consists mostly of light from the host galaxy. For these reasons, this candidate could not be typed, and C.I. was not assigned.

3.3.5. SCP06G4

The spectrum of SCP06G4 is shown in figure 14. It was taken on 2006 April 22 and 23, and the total integration was 22800 s. SCP06G4 is well separated from the putative host galaxy, which lies to the northeast of SCP06G4. The redshift of the host is $z_{\rm gal} \sim 1.35$ from Ca II H and K absorption lines and the 4000Å break. A spectral fit to the host galaxy resulted in a similar redshift, $z_{\rm gal} = 1.350$ (see section 4).

Although SCP06G4 is well separated from the host galaxy in the ACS images, the SN spectrum was strongly contaminated by light from the host galaxy. Thus, we subtracted a spectrum that was extracted from a location that was at the same distance from the galaxy center to the SN, but on the other side of the galaxy. The host subtracted spectrum of SCP06G4 is very noisy, and could be fitted with a SN Ib/c template at $t = -6$ days redshifted to $z_{\rm SN} = 1.36$ or the Hsiao Ia template at $t = -1$ days redshifted to $z_{\rm SN} = 1.35$. Host galaxy subtraction using the BC03 templates also gave the best-fitting result of $t = -1$ days redshifted to $z_{\rm SN} = 1.35$ (the upper panel of figure 14). The light curve is consistent with that of a SN Ia, and $t_{\rm sp}$ matches $t_{\rm LC}$. The C.I. is 3. The classification is supported by the characteristics of the host galaxy. The morphology of the host is consistent with it being an elliptical galaxy (J. Meyers et al. in preparation), and no [O II] emission has been detected in the spectrum of the host.

SCP06G4 is the most distant spectroscopically confirmed SN Ia in our sample, and the most distant spectroscopically confirmed SN Ia using a ground-based telescope. The confidence in the classification is similar to that which can be

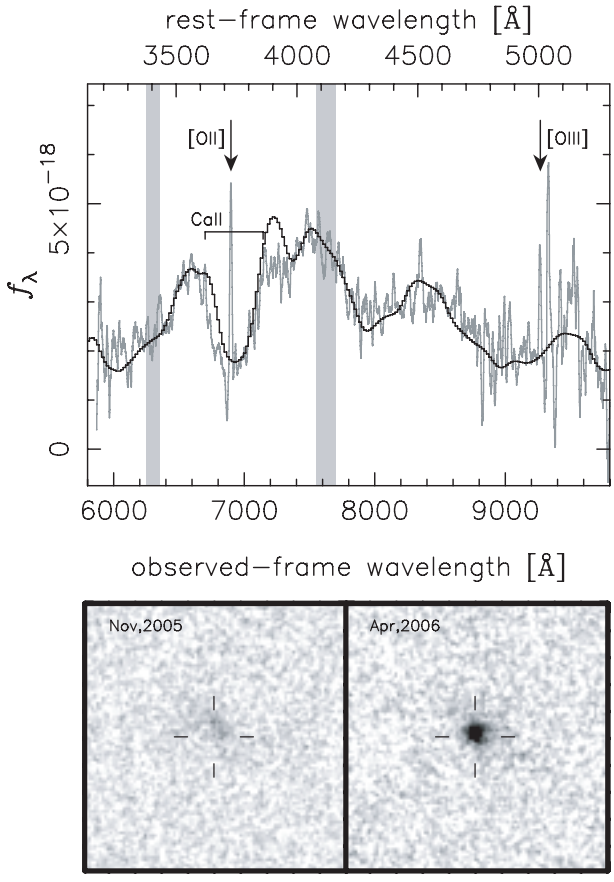

Fig. 15. (top): Spectrum of SCP06H3 at $z_{\rm gal} = 0.851$ (gray) and the Hsiao Ia template at $t = 2$ days redshifted to $z_{\rm SN} = 0.84$ (black). The C.I. is 4. (bottom): Finding charts of SCP06H3.

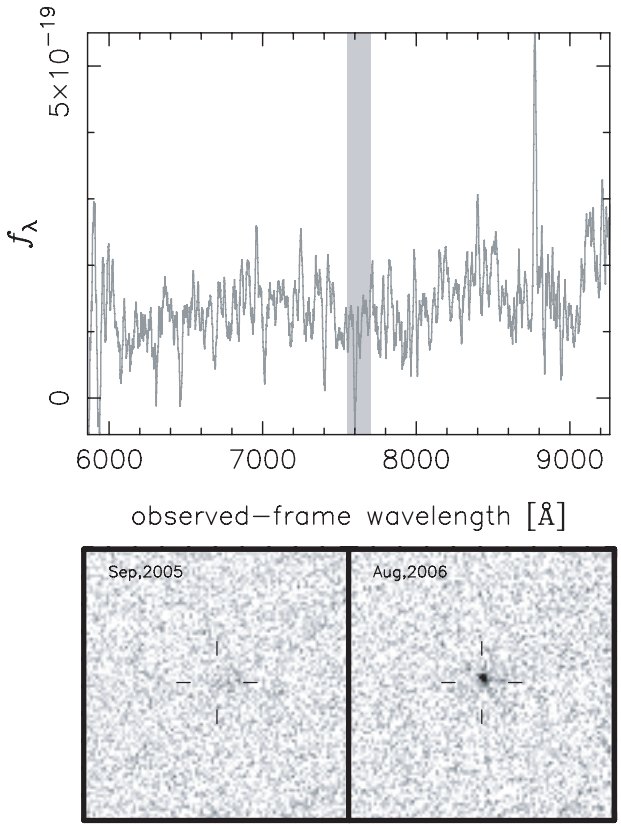

Fig. 16. (top): Spectrum of SCP06N32. The C.I. is 2. (bottom): Finding charts of SCP06N32.

obtained for other similarly distant SNe that have ACS grism spectra (Riess et al. 2007). Clearly, in some cases, one can do as well from the ground as from space, if the atmospheric conditions are optimal, the host either faint enough or far enough away from the SN, integrations are long, and some care in adopting the optimal observing and data reduction strategies are employed.

3.3.6. SCP06H3

The spectrum of SCP06H3 is shown in figure 15. It was taken on 2006 April 22, and the total integration time was 6000 s. SCP06H3 appears to be associated with a very diffuse galaxy. The redshift of the galaxy is $z_{\rm gal} = 0.851$, as measured from [O II] and [O III]. The spectrum of SCP06H3 was well-fitted to the Hsiao Ia template at $t = 2$ days redshifted to $z_{\rm SN} = 0.84$. The light curve is consistent with that of a SN Ia, and $t_{\rm sp}$ matches $t_{\rm LC}$, so C.I. is set to 4.

3.3.7. SCP06N32

The spectrum of SCP06N32 is shown in figure 16. It was taken on 2006 August 22, and the total integration time was 7200 s. SCP06N32 appears to be associated with a very diffuse and faint galaxy. We did not detect any spectral features from the galaxy. Although broad features were visible, the spectrum is noisy and the fitting results are inconclusive. The C.I. is set to 2.

3.3.8. SCP05P1

The spectrum of SCP05P1 is shown in figure 17. It was taken on 2005 September 25, and the exposure time was 5400 s. SCP05P1 appears near to the center of a very diffuse galaxy, which has a redshift of $z_{\rm gal} = 0.926$ from a [O II] emission line. Since the spectrum was taken $t \sim 15$ days after the light curve peak, we restrict the spectral fits to late SN epochs. The best fit spectral template is SN 1998S, a Type IIn SN, at $t = 27$ days redshifted to $z_{\rm SN} = 0.91$, but the fit is poor. Allowing for some host galaxy light in the spectrum did not lead to a more conclusive fit. Since the spectrum was taken more than two weeks after maximum light, the confidence index is left unassigned.

3.3.9. SCP05P9

The spectrum of SCP05P9 is shown in figure 18. It was taken on 2005 October 25, and the exposure time was 12600 s. SCP05P9 is well separated from a galaxy that has a redshift of $z_{\rm gal} = 0.821$, as measured from a [O II] emission line. The host galaxy is located northwest of SCP05P9 in the finding chart of figure 18. The separation of the SN component from the host galaxy center is about 1 arcsec and, as in SCP06G4, we subtracted the host galaxy component from the spectrum at the SN position (sub-subsection 3.3.5). The best-fit template over the observed wavelength range is the Hsiao Ia template at $t = -2$ days at $z_{\rm SN} = 0.81$. The light curve is consistent with that of a SN Ia, and $t_{\rm LC}$ matches $t_{\rm SN}$. C.I. is 3.

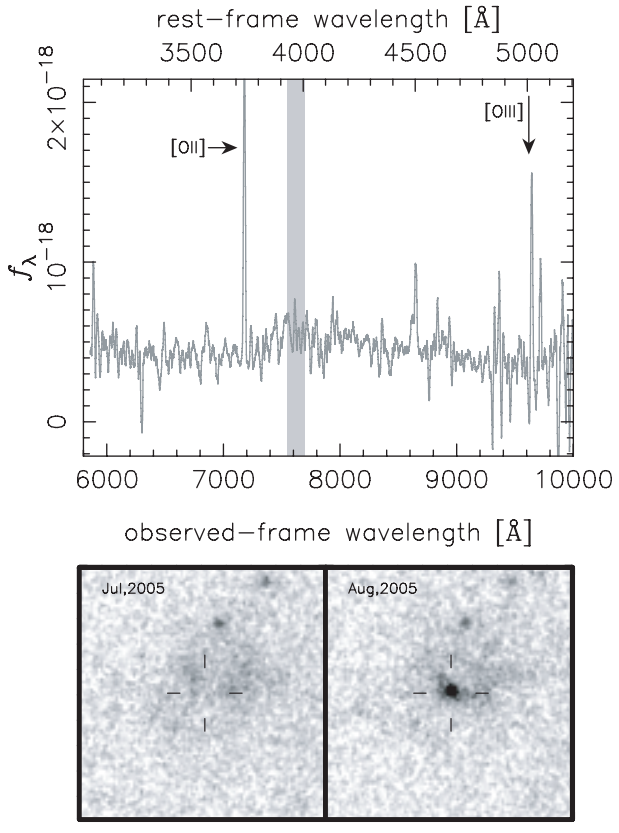

Fig. 17. (top): Spectrum of SCP05P1 at $z_{\rm gal} = 0.926$ (gray). The C.I. is 2. (bottom): Finding charts of SCP05P1.

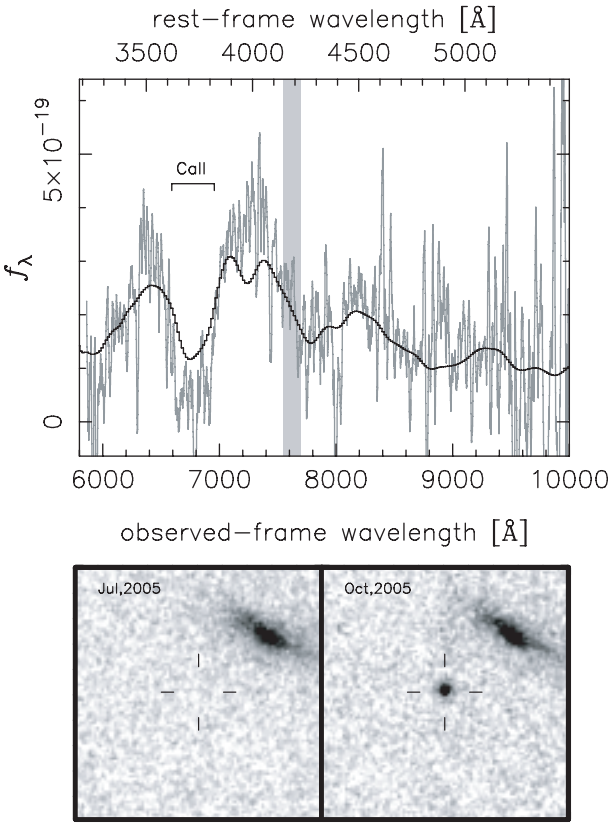

Fig. 18. (top): Spectrum of SCP05P9 at $z_{\rm gal} = 0.821$ (gray) and the Hsiao Ia template at $t = -2$ days redshifted to $z_{\rm SN} = 0.81$ (black). We note that we determine the redshift from the spectrum of the host galaxy center, and the [O II] emission line can not be seen in the SN spectrum figure. C.I. is 3. (bottom): Finding charts of SCP05P9.

4. Host Galaxy Spectral Fitting for SN Candidates in HST Cluster Supernova Survey

As an alternative to spectroscopy, classification of the SN from other observables, such as the lightcurve or the properties of the host can, and sometimes must, be employed. Identifying the host of a SN as an early type galaxy is a reasonable indication that the SN is a SN Ia, as SNe of other types are unlikely to occur in such galaxies. We fitted BC03 models to the hosts of five SN candidates in HST Cluster Supernova Survey to constrain the spectral properties of the hosts. The parameters of the fit were metallicity, star-formation history (single burst or exponentially declining), star-formation time scale, $\tau_{\rm sf}$, stellar age, $t_{\rm age}$, and extinction. In the fitting, we masked the region covering the atmospheric A-band around 7600Å and any possible emission lines, since the BC03 models do not reproduce non-stellar spectral features. The spectral fitting also allowed a more accurate estimate of the redshifts of those host galaxies for which the Ca II H and K absorption lines were detected with a low signal-to-noise ratio.

The FOCAS spectra of the hosts of SCP05D0, SCP05D6, SCP06G4, SCP06K0, and SCP06K18 and the best-fitting galaxy spectra are shown in figures 19–23. We note that SCP06G4 is spectroscopically identified as a SN Ia* (subsubsection 3.3.5). Observations for these host galaxies are summarized in tables 2 and 3. In general, the contribution from the SN in these spectra can be ignored. SCP05D0, SCP05D6, SCP06K0, SCP06K18 were all re-observed when the contribution from the SN was negligible. For SCP06G4, a spectrum located at the center of the host was extracted. While some SN light may have leaked into the slit for these two objects, the contribution was estimated to be negligible for SCP06G4.

All of the observed galaxy spectra were well-fitted with the models from BC03. Using the constraint that the age of the universe at the redshifts the galaxies were observed (for example, 6.0 Gyr at $z \sim 1.0$ and 4.7 Gyr at $z \sim 1.4$) should be larger than the respective ages of these galaxies, we obtained ranges (among the 40 best-fitted templates) for the stellar age, $t_{\rm age}$, and the star-formation time scale, $\tau_{\rm sf}$, for each galaxy. The uncertainties are large because the observed spectra are noisy. The 40 best-fitted templates provide roughly the same χ^2 values. The stellar ages, $t_{\rm age}$, are larger than the timescales of star formation, $\tau_{\rm sf}$, for all galaxies. Among the well-fitted templates, templates with older ages generally have smaller extinction than those of younger ages. From our spectral fitting, we cannot exclude the possibility of significant extinction, but all of the spectra are consistent with early-type galaxies with little extinction. The above results are summarized in table 4.

Table 4. Spectral fitting results for SN hosts.*

SN	$z_{\rm gal}$	$z_{\rm gal,fit}$	$t_{\rm age}$ [Gyr]	$\tau_{\rm sf}$ [Gyr]	Ca II H and K	4000Å break
SCP05D0	1.015	1.015	1.0–3.0	0.0–0.5	clear	clear
SCP05D6	1.315	1.316	1.5–3.0	0.0–0.1	clear	clear
SCP06G4	$\sim$1.35	1.350	1.0–1.5	0.0–0.3	exist	clear
SCP06K0	$\sim$1.41	1.416	1.5–3.0	0.0–0.3	exist	clear
SCP06K18	$\sim$1.41	1.411	1.5–3.0	0.0–0.5	exist	clear

* The SN names are denoted in column 1. Columns 2 and 3 contain the redshifts measured from individual spectral features, some of which are not very precise due to the noisy nature of the spectra, and the redshifts derived from the spectral fitting, respectively. Columns 4 and 5 contain the fitted ranges of ages and star formation timescales. Both are in Gyr. In columns 6 and 7, the qualitative strengths of the Ca II H and K absorption lines and the 4000Å break are shown, respectively.

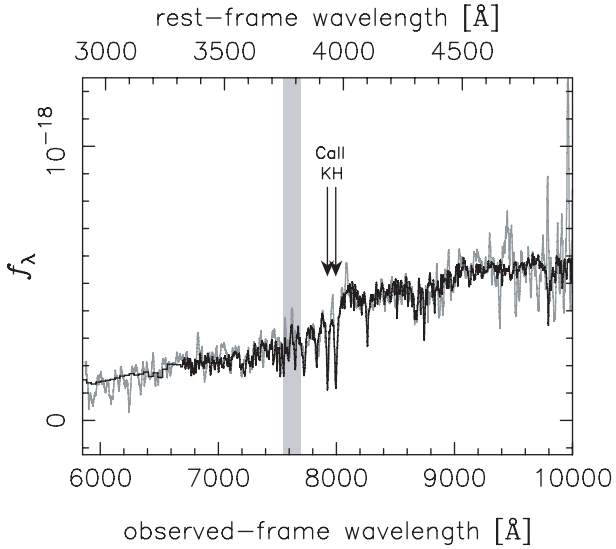

Fig. 19. Spectrum of the host of SCP05D0 (gray) and the best-fitting galaxy template at $z_{\rm gal,fit} = 1.015$ (black).

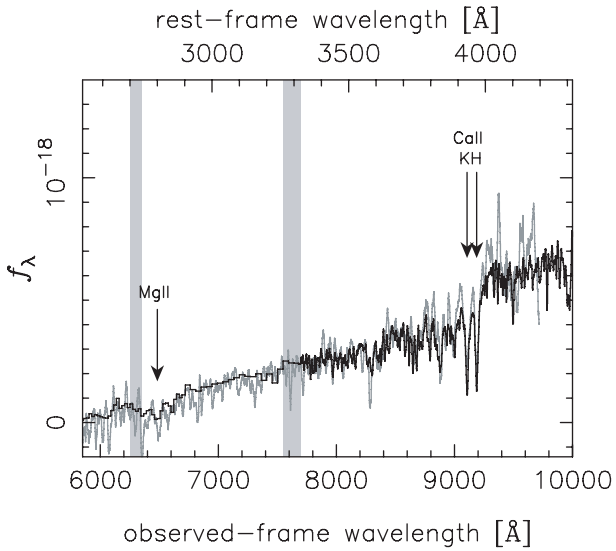

Fig. 20. Spectrum of the host of SCP05D6 (gray) and the best-fitting galaxy template at $z_{\rm gal,fit} = 1.316$ (black).

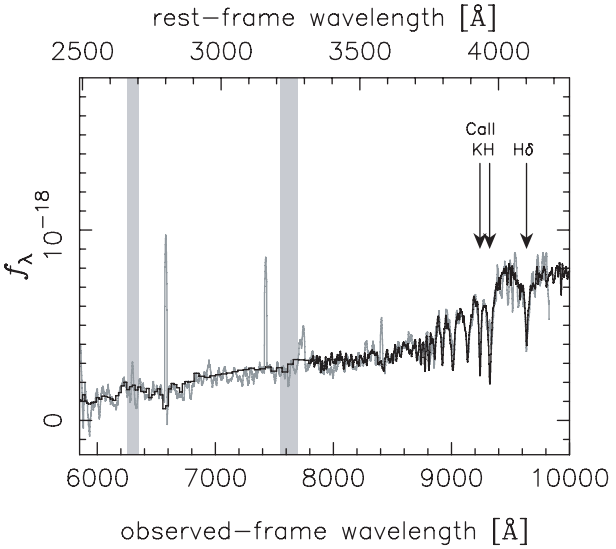

Fig. 21. Spectrum of the host of SCP06G4 (gray) and the best-fitting galaxy template at $z_{\rm gal,fit} = 1.350$ (black).

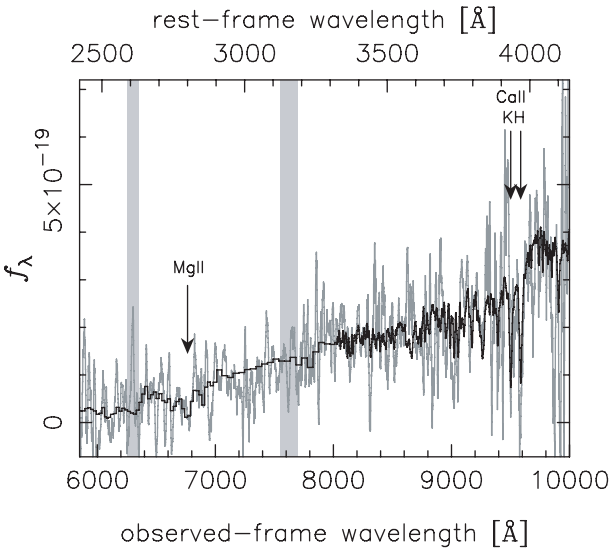

Fig. 22. Spectrum of the host of SCP06K0 (gray) and the best-fitting galaxy template at $z_{\rm gal,fit} = 1.416$ (black).

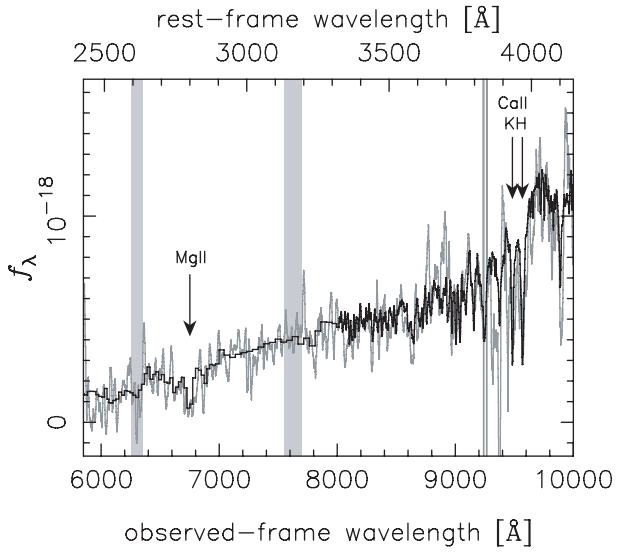

Fig. 23. Spectrum of the host of SCP06K18 (gray) and the best-fitting galaxy template at $z_{\rm gal,fit} = 1.411$ (black).

5. Classifying High-Redshift Candidates

The chance that any given high-redshift candidate is positively identified as a SN of some type depends on many factors. A non-exhaustive list includes factors like the redshift of the candidate, the phase at which it was observed, the contrast with respect to the host, the wavelength coverage and the signal-to-noise ratio of the spectrum, and, if photometry is used as part of the classification, the quality and amount of photometry. The lack of a large sample of UV spectra for SNe of all types, especially for CC SNe, is also a factor.

In figures 24 and 25 we compare the magnitudes, redshifts and signal-to-noise ratios of candidates that were successfully identified with those that were not. Only candidates that were observed within about two rest-frame weeks of the maximum light are included in these plots. The signal-to-noise ratios include both the SN and the host-galaxy components, except for SCP06G4 and SCP05P9, for which we subtracted the spectrum of the host. Although the exposure times and weather conditions differed from one candidate to the next, one generally finds, not surprisingly, that it is easier to identify the SN type when they were at lower redshift, when they were brighter and when the signal-to-noise of the spectrum was higher.

Also critical is the phase of the SN when the spectrum was taken. In figure 26, $t_{\rm LC}$ (the light-curve epoch at the time the spectrum was taken) is plotted as a function of the redshift. Only objects with well-sampled light curves are shown, so objects like CL1604_0-1 and SDF1 were excluded. Black circles and boxes are SNe that have a C.I. greater than 2. Considering only the spectra within the shaded region, 5 out of 11 candidates observed with FOCAS were spectroscopically identified as SN Ia or SN Ia*. Of these 5, 4 are below $z = 1.1$. To increase the number of candidates in this comparison, we added 8 SN candidates from the HST Cluster Supernova Survey (Dawson et al. 2009) that were observed with FORS2: SCP06A4, SCP06C0, SCP06C1, SCP05D0,

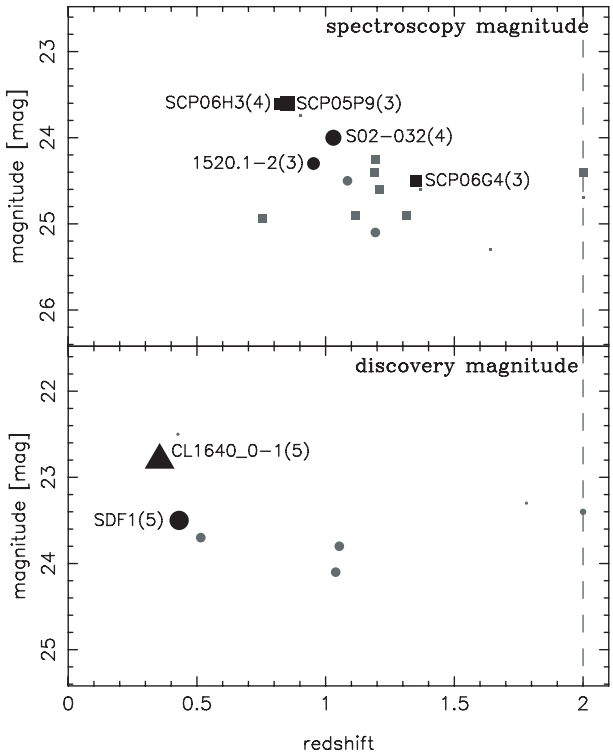

Fig. 24. Distribution of SN candidate magnitudes as a function of the redshift. If a sufficient well sampled lightcurve is available, the magnitude at the time the spectrum was taken was used, and is shown in the upper panel. Otherwise, the magnitude at the time of discovery was used, and is shown in the lower panel. The symbol size is proportional to the degree of confidence that the candidate is a SN Ia. We plot candidates with C.I. ≤ 2 in gray. Triangle, circles and boxes represent R_c, i', and z'–magnitudes, respectively. Symbols on the vertical gray dashed line at $z = 2$ are objects whose redshifts could not be determined.

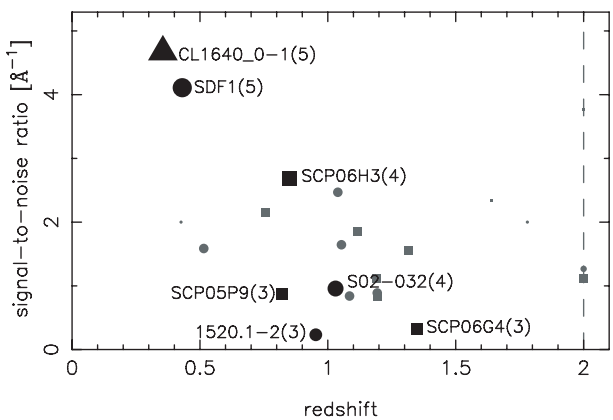

Fig. 25. Distribution of the signal-to-noise ratios of the spectra as a function of the redshift. Symbols are the same as those in figure 24. For SCP05P9 and SCP06G4, we plot the signal-to-noise ratios of the host-subtracted SN component spectra. Symbols on the vertical gray dashed line at $z = 2$ are objects whose redshifts could not be determined. For reference, a 2-hour, low resolution ($R \sim 500$) spectrum with FOCAS of a $z' \sim 25$ mag point source has S/N = 1 [Å^{-1}]. The signal-to-noise ratios are not scaled to a common exposure time. Doing so tends to stretch the plot vertically.

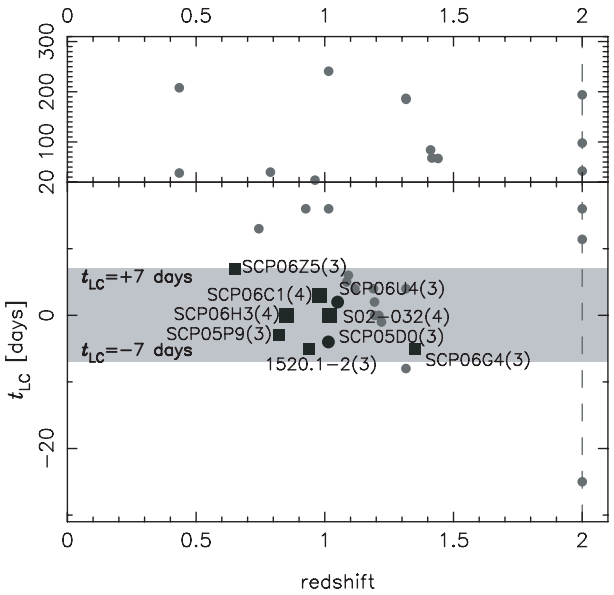

Fig. 26. Distribution of the epoch the spectra taken as a function of the redshift. We only consider objects with well-sampled light curves that have a well-determined date of peak brightness. Circles indicate candidates that we could only identify as a SN Ia when a spectrum of the host was available. The gray region is $-7 \leq t_{\rm LC} \leq 7$ days. We note that circles at $z = 2$ are objects without a spectroscopic redshift determination, and we plot the observed-frame epochs for these objects. The object at $t_{\rm LC} \sim -25$ days is the extraordinary transient SCP06F6.

SCP05D6, SCP06R12, SCP06U4, and SCP06Z5. Considering only the spectra within the shaded region, and combining the results from FOCAS and FORS2, 9 out of 18 candidates (50%) were spectroscopically identified as SN Ia or SN Ia*. Of these 9, 8 are below $z = 1.1$. FORS2 and FOCAS proved to be equally effective in this redshift interval.

Clearly, $z > 1.1$ SNe Ia are more difficult to confirm spectroscopically with ground-based facilities. This is not a surprising result. They are fainter and the peak of the flux is shifted into a wavelength region where the night sky is bright. However, it is possible to confirm SNe beyond $z = 1.1$ with optical instrumentation, if the conditions are ideal and integrations are long. SCP06G4 in this paper is an example. With the upgrade of optical spectrographs with CCDs that have improved the red sensitivity and minimal fringing (as was recently done for LRIS on Keck and is now being done for FOCAS on Subaru), it should be possible to increase the yield of spectroscopically classified SNe Ia with ground-based facilities beyond $z = 1.1$. Laser guide star adaptive optics (LGS-AO) assisted infra-red spectroscopy may be another alternative; however, only a few SNe Ia are expected to have a tip-tilt star that is both near enough and bright enough for LGS-AO to be effective. SCP05D6, for example, was imaged in the H-band (rest frame R-band) with the LGS-AO system at the Keck Observatory (Melbourne et al. 2007).

The strategy adopted in the HST Cluster SN Survey is an alternative. Since Type II SN are extremely rare in early-type galaxies, a spectroscopic confirmation of the SN type in such galaxies is unnecessary. Spectroscopy is still necessary to obtain redshifts. However, the amount of time needed to obtain redshifts is generally much less than that needed to confirm the SN type, and the spectrum can be taken long after the SN is no longer visible. In one case, SCP05D0, the spectrum of the host was available from archived data, and was taken before the SN exploded (Dawson et al. 2009). The key here is to show that the amount of star formation in the host is low enough that the SN of other types are unlikely.

6. Summary

We have presented spectra of SN candidates obtained with FOCAS on the Subaru 8.2-m telescope. Seven active candidates were identified as SNe Ia, including SCP06G4 at $z_{\rm SN} = 1.35$, the most distant SN Ia to be spectroscopically identified with a ground-based telescope. Redshifts were obtained for all but 7 of the remaining 32 candidates based on the host galaxy spectra. An additional 4 candidates were identified as likely SNe Ia from the spectrophotometric properties of their hosts. The spectral properties of these hosts found in the HST Cluster Supernova Survey were examined by comparing their spectra with the BC03 model spectra. All of the host galaxy spectra indicate that they are passively evolving galaxies that have quenched their star-forming activities.

We also investigated the factors affecting the classification of SNe, and found that it is critical to take spectra within one week of the maximum light. This requires secure early detection, well-sampled light curves and a prompt spectroscopic follow-up.

We thank an anonymous referee for providing helpful comments and suggestions. TM and YI are financially supported by the Japan Society for the Promotion of Science (JSPS) through the JSPS Research Fellowship. CL acknowledges the financial support from the Oskar Klein Centre at the University of Stockholm. This work was supported in part by scientific research grants (Nos. 15204012 and 17104002) from the Ministry of Education, Science, Culture, and Sports of Japan, and a JSPS core-to-core program "International Research Network for Dark Energy". Financial support for this work was provided in part by NASA through program GO-10496 from the Space Telescope Science Institute, which is operated by AURA, Inc., under NASA contract NAS 5-26555. This work was also supported in part by the Director, Office of Science, Office of High Energy and Nuclear Physics, of the U.S. Department of Energy under Contract No. AC02-05CH11231. Part of the Suprime-Cam observations were made during the guaranteed time observation of Suprime-Cam, and we thank for the Suprime-Cam instrument team. We also appreciate much help by the SDF and SXDS project team members. We thank Youichi Ohyama, who helped our observations as a support scientist of FOCAS. Data analysis were in part carried out on a common-use data analysis computer system at the Astronomy Data Center, ADC, of the National Astronomical Observatory of Japan.

References

Aldering, G., et al. 1998, IAU Circ., 7046, 1
Aldering, G., et al. 2002, Proc. SPIE, 4836, 61
Amanullah, R., et al. 2009, ApJ submitted
Astier, P., et al. 2006, A&A, 447, 31
Barbary, K., et al. 2009, ApJ, 690, 1358
Barris, B. J., et al. 2004, ApJ, 602, 571
Benítez, N., et al. 2003, Rev. Mex. Astron. Astrofis., 16, 39
Bruzual, G., & Charlot, S. 2003, MNRAS, 344, 1000
Cardelli, J. A., Clayton, G. C., & Mathis, J. S. 1989, ApJ, 345, 245
Coil, A. L., et al. 2000, ApJ, 544, L111
Cuillandre, J.-C., Luppino, G. A., Starr, B. M., & Isani, S. 2000, Proc. SPIE, 4008, 1010
Dawson, K., et al. 2006, Cent. Bur. Electron. Telegrams, 546, 1
Dawson, K. S., et al. 2009, AJ, 138, 1271
Doi, M., et al. 2001, IAU Circ., 7649, 1
Doi, M., et al. 2003, IAU Circ., 8119, 1
Eisenhardt, P. R. M., et al. 2008, ApJ, 684, 905
Eisenstein, D. J., et al. 2005, ApJ, 633, 560
Frieman, J. A., et al. 2008, AJ, 135, 338
Hamuy, M., et al. 2006, PASP, 118, 2
Hicken, M., et al. 2009, ApJ, 700, 1097
Hodapp, K. W., et al. 2003, PASP, 115, 1388
Howell, D. A., et al. 2005, ApJ, 634, 1190
Hsiao, E. Y., et al. 2007, ApJ, 663, 1187
Iwamuro, F., Motohara, K., Maihara, T., Hata, R., & Harashima, T. 2001, PASJ, 53, 355
Jha, S., et al. 2006, AJ, 131, 527
Kashikawa, N., et al. 2002, PASJ, 54, 819
Kashikawa, N., et al. 2004, PASJ, 56, 1011
Komatsu, E., et al. 2009, ApJS, 180, 330
Lidman, C., et al. 2005, A&A, 430, 843
Lubin, L. M., Mulchaey, J. S., & Postman, M. 2004, ApJ, 601, L9
Melbourne, J., et al. 2007, AJ, 133, 2709
Miknaitis, G., et al. 2007, ApJ, 666, 674
Miyazaki, S., et al. 2002, PASJ, 54, 833
Moorwood, A., et al. 1998, The Messenger, 94, 7
Morokuma, T., et al. 2008, ApJ, 676, 163
Motohara, K., et al. 2002, PASJ, 54, 315
Nugent, P., Kim, A., & Perlmutter, S. 2002, PASP, 114, 803
Oda, T., & Totani, T. 2005, ApJ, 630, 59
Oda, T., Totani, T., Yasuda, N., Sumi, T., Morokuma, T., Doi, M., & Kosugi, G. 2008, PASJ, 60, 169
Perlmutter, S., et al. 1999, ApJ, 517, 565
Phillips, M. M. 1993, ApJ, 413, L105
Riess, A. G., et al. 1998, AJ, 116, 1009
Riess, A. G., et al. 2004, ApJ, 607, 665
Riess, A. G., et al. 2007, ApJ, 659, 98
Sako, M., et al. 2008, AJ, 135, 348
Sekiguchi, K., et al. 2004, BAAS, 205, 8105
Spergel, D. N., et al. 2003, ApJS, 148, 175
Spergel, D. N., et al. 2007, ApJS, 170, 377
Stocke, J. T., et al. 1991, ApJS, 76, 813
Takanashi, N., Doi, M., & Yasuda, N. 2008, MNRAS, 389, 1577
Tanaka, M., et al. 2008, A&A, 489, 571
Thompson, R. I., et al. 1999, AJ, 117, 17
Tokita, K. 2009, Ph.D. Thesis, The Univ. of Tokyo
Tonry, J. L., et al. 2003, ApJ, 594, 1
Totani, T., Sumi, T., Kosugi, G., Yasuda, N., Doi, M., & Oda, T. 2005, ApJ, 621, L9
Totani, T., Morokuma, T., Oda, T., Doi, M., & Yasuda, N. 2008, PASJ, 60, 1327
Tripp, R. 1998, A&A, 331, 815
Vikhlinin, A., et al. 2009, ApJ, 692, 1060
Wood-Vasey, W. M., et al. 2007, ApJ, 666, 694
Yasuda, N., et al. 2002, IAU Circ., 7971, 2
Yasuda, N., et al. 2003, BAAS, 203, 8211
Zheng, C., et al. 2008, AJ, 135, 1766